Biochemical Pharmacology 247 (2026) 117766

Contents lists available at ScienceDirect

Biochemical Pharmacology

journal homepage: www.elsevier.com/locate/biochempharm

A *Vibrio*-susceptibility class of antimicrobial peptide Ajapocin via membranolytic pattern to combat "non-cholera" pathogens *in vivo* infection models

Xiaofei Wang [a,1], Xiao Hong [a,1], Wanting Liu [b], Yujun Xu [a], Roushi Chen [a], Fangyi Chen [a,c,d], Ke-Jian Wang [a,c,d,*], Luxi Wang [b,**]

[a] State Key Laboratory of Marine Environmental Science, College of Ocean & Earth Sciences, Xiamen University, Xiamen, Fujian, China
[b] Department of Psychiatry and Department of Physiology, Sir Run Run Shaw Hospital School of Medicine, Zhejiang University, Hangzhou, Zhejiang, China
[c] State-Province Joint Engineering Laboratory of Marine Bioproducts and Technology, College of Ocean & Earth Sciences, Xiamen University, Xiamen, Fujian, China
[d] Innovation Research Institute for Marine Biological Antimicrobial Peptide Industry Technology, Fujian Ocean Innovation Center, Xiamen, Fujian, China

ARTICLE INFO

Keywords:
Antimicrobial peptide
Non-cholera pathogens
Ajapocin
Anti-*Vibrio*infection

ABSTRACT

Pathogenic "non-cholera" *Vibrio* species of *Vibrio parahaemolyticus* (*V. parahaemolyticus*) and *Vibrio vulnificus* (*V. vulnificus*) frequently pose a serious threat to aquaculture security and public health by causing infectious diseases. In this study, we reported the discovery of a marine-sourced antimicrobial peptide (AMP) called Ajapocin, which identified through a sequence optimization strategy. Ajapocin exhibited potent activity against *V. parahaemolyticus* and *V. vulnificus* pathogens, with minimum inhibitory concentrations (MICs) of 6–12 μM—comparable to the clinical agent Polymyxin B (PMB). *In vivo*, a single administration of Ajapocin (1 mg/mL) displayed therapeutic efficacy in a zebrafish-*Vibrio* infection model. Multiple doses reduced bacterial burden and accelerated wound healing in a mouse model of *V. vulnificus*-infected skin wounds. Ajapocin showed no cytotoxicity in ZF4 cells and HaCaT cells at concentrations up to 32 μM. Notably, after intraperitoneal injection for 1 week, Ajapocin did not induce cumulative hepatic or renal toxicity, as confirmed by histopathology analysis and chemistry profiles. Mechanistically, membrane-interacting Ajapocin targeted negative cellular components, enhancing membrane permeation, inducing membrane depolarization, and ultimately causing membrane damage and bacterial dysfunction. Taken together, these results position Ajapocin as an appealing anti-*Vibrio* agent for combating vibriosis in both aquaculture and clinical settings.

Abbreviations: MDR, Multi-drug resistant; MICs, Minimum inhibitory concentrations; AMPs, Antimicrobial peptides; *V. parahaemolyticus*, *Vibrio parahaemolyticus*; *V. vulnificus*, *Vibrio vulnificus*; CLSI, Clinical and Laboratory Standard Institute; PMB, Polymyxin B; HPLC, High-performance liquid chromatography; MS, Mass spectrometry; SPPS, Solid-phase peptide synthesis; NPN, 1-N-phenylnaphthylamine; PI, Propidium iodide; DAPI, 4′,6-diamidino-2-phenylindole; LPS, Lipopolysaccharide; CL, Cardiolipin; PC, Phosphatidylcholine; $DiSC_3(5)$, 3,33,3′-diapropylthiadicarbocyanine iodide; CGMCC, China General Microbiological Culture Collection Center; ATCC, American Type Culture Collection; CDC, Centers for disease control and prevention; TSB, Tryptic soy broth; MHB, Mueller-Hinton broth; BSA, Bovine serum albumin; HBSS, Hanks' balanced salt solution; FBS, Fetal bovine serum; DMEM, Dulbecco's modified Eagle medium; DMEM/F-12, Dulbecco's modified Eagle medium/nutrient mixture F-12; IVCs, Individually ventilated cages; IACUC, Institutional Animal Care and Use Committee; CFUs, Colony-forming units; CCK-8, Cell counting kit-8; SEM, Scanning electron microscopy; TEM, Transmission election microscopy; CLSM, Confocal laser scanning microscopy; NaPB, Sodium phosphate buffer; PBS, Phosphate-buffered saline; pI, Isoelectric point; ALT, Alanine aminotransferase; AST, Aspartate aminotransferase; BUN, Urea nitrogen; CRE, Creatinine; ANOVA, One-way analysis of variance; SD, Standard deviation; e.g., Exempli gratia; H&E, Hematoxylin and eosin; a.u., Arbitrary unit; DIC, Differential interference contrast; OD, Optical density.

* Corresponding author at: State Key Laboratory of Marine Environmental Science, College of Ocean & Earth Sciences, Xiamen University, Xiamen, Fujian, China.
** Corresponding author.
E-mail addresses: wkjian@xmu.edu.cn (K.-J. Wang), luxiwang@zju.edu.cn (L. Wang).
[1] These authors contributed equally to this work.

https://doi.org/10.1016/j.bcp.2026.117766
Received 17 November 2025; Received in revised form 27 January 2026; Accepted 27 January 2026
Available online 1 February 2026

1. Introduction

Vibrio species are Gram-negative bacteria that originate from aquatic and marine habitats [1,2]. Among them, the non-cholera pathogens of *V. parahaemolyticus* and *V. vulnificus* are particularly important as they cause severe infections in aquatic organisms and are recognized as major environmental human pathogens [3–5]. In addition to their opportunistic nature, epidemiological surveys indicate that approximately 12 % of *Vibrio* species are capable of causing human infections [1]. Alarmingly, the prevalence of antibiotic-resistant *Vibrio* strains has increased substantially over recent decades, resulting in several vibriosis diseases and clinical manifestations [6,7]. Without effective treatment, *Vibrio* infections can rapidly progress to life-threatening conditions. Consequently, there is an urgent need for potent antibacterial agents capable of eradicating these highly virulent pathogens, highlighting the importance of developing practical and targeted strategies against *Vibrio* spp. infections.

AMPs are distributed across various species and play pivotal roles to combat invading pathogenic bacteria [8,9]. These peptides exhibit diverse mechanisms of action, making them promising candidates against antibiotic-resistant *Vibrio* strains [10,11]. However, *Vibrio* species thrive under halophilic conditions, which often compromise the efficacy of many conventional AMPs in high salt environments [12,13]. To overcome this limitation, AMPs derived from marine invertebrate phyla have gained attention [14–19], as they are naturally adapted to saline conditions and may retain strong activity in such environments [17,19–21]. Additionally, AMPs from marine invertebrates typically featured cationic and hydrophobic properties [19], which are critical for effectively targeting key components of microbial membranes [19,22]. Accordingly, we focused on certain marine species possessing innate immune systems exclusively, as we hypothesized that peptides derived from these organisms might display stronger antimicrobial activity or greater tolerance to high salt concentrations [14]. Despite the growing awareness of *Vibrio* infections, studies on anti-*Vibrio* AMPs remain limited. Therefore, identifying and characterizing salt-tolerant AMPs with potent vibriocidal activity is of great significance for advancing therapeutic strategies against *Vibrio* infections.

To discover superior anti-*Vibrio* agents, we initiated a screening strategy targeting the sea cucumber *Apostichopus japonicus* based on genomic data [23,24]. Our approach integrated a structure–activity-guided design, and supported by an analysis of general physicochemical properties desirable for AMPs-appropriate peptide length, modest positive charge and balanced hydrophobicity [8]. Additionally, we performed AMP optimization by mining reported AMP databases [25,26]. This process led to the identification of a previously unexploited lead peptide, termed Ajapocin, which was characterized for the first time in this study. Both its physical and chemical parameters were highly similar to those of identified AMPs, and predictive analysis indicated that Ajapocin possessed helicity by adopting an α–helical structure. Next, we conducted two distinct assays to validate its potent anti-*Vibrio* activity and rapid killing efficiency. Importantly, a prodrug strategy was developed to enhance the *in vivo* efficacy of Ajapocin, which was evaluated using both a zebrafish infection model and a murine wound infection model. Furthermore, we thoroughly discussed the mechanism of action of Ajapocin underlying membrane disruption profiles, which were implicated in enhancing membrane permeability and inducing membrane depolarization. The *in vitro* safety of Ajapocin was confirmed using cellular models, and its cumulative toxicity *in vivo* was assessed via multiple administrations for 1 week. In conclusion, our current study presents a promising AMP-based strategy for addressing *Vibrio* spp. -infections.

2. Materials and methods

2.1. Peptide synthesis and antibiotic preparation

Peptides were synthesized via standard solid-phase peptide synthesis (SPPS) methods using rink amide AM resin. The process involved sequentially amino-acid coupling reactions followed by cleavage from the resin using trifluoroacetic acid. After acquiring raw peptides, all of them were further processed in common C-terminal modification with amidation. Peptide purity of $>$ 95 % was achieved, as determined by the combination with mass spectrometry (MS) and high-performance liquid chromatography (HPLC) technologies. Finally, peptide products-including Ajapocin (GFRIAFKRILTCGKK), FITC-Ajapocin, Spgillcin$_{177-189}$ and Melittin-were provided by GL Biochem (Shanghai, China). Antibiotic PMB sulfate was purchased from Solarbio (Beijing, China). Both peptides and antibiotic stock solutions were freshly prepared by dissolving in sterile Milli-Q water.

2.2. Chemical Reagents

The fluorescent dye 1-N-phenylnaphthylamine (NPN), the apoptotic dye propidium iodide (PI), the nuclei dye 4′,6-diamidino-2-phenylindole (DAPI), the lipopolysaccharide (LPS), the phospholipid cardiolipin (CL) and phosphatidylcholine (PC) were purchased from Sigma-Aldrich (Missouri, USA). LIVE/DEAD™ *Bac*light bacterial viability kit was purchased from Invitrogen (California, USA), the fluorescent probe 3,33,3′-diapropylthiadicarbocyanine iodide [DiSC$_3$(5)] was purchased from Aladdin (Shanghai, China).

2.3. Bioinformatic analysis

The physical and chemical parameters of Ajapocin including molecular weight, theoretical isoelectric point (pI), net charge and hydrophobicity were calculated through the ExPASy Bioinformatics Resource Portal (http://www.expasy.org/tools/). Its helix-wheel structure was generated using HeliQuest website (https://heliquest.ipmc. cnrs.fr/), and the three-dimensional projection was predicted using I-TASSER (http://zhanglab.ccmb.med.umich.edu/I-TASSER/).

2.4. Bacterial strains and cell lines

The *Vibrio* strains of *V. parahaemolyticus* ATCC 17802 and *V. vulnificus* were included in this study. *V. parahaemolyticus* ATCC 17802 was purchased from China General Microbiological Culture Collection Center (CGMCC, Beijing, China), and the *V. vulnificus* strain was kindly provided by the Haid group (Guangdong, China), having been isolated and purified from aquatic environments. All strains were cultured in Tryptic soy broth (TSB) medium (Qingdao, China) containing 2 % NaCl. HaCaT cells and ZF 4 cells were obtained from the American Type Culture Collection (ATCC, Virginia, USA), HaCaT cells were cultivated in Dulbecco's modified Eagle medium (DMEM) supplemented with 10 % fetal bovine serum (FBS) and 1 % (w:v) penicillin–streptomycin (Solarbio, Beijing, China) at 37 ℃ in a 5 % CO_2 atmosphere. ZF4 cells were maintained in Dulbecco's modified Eagle medium/nutrient mixture F-12 medium (DMEM/F-12) supplemented with 10 % FBS, and 1 % penicillin–streptomycin at 28°C in humidified atmosphere with 5 % CO_2.

2.5. Animals

2.5.1. Zebrafish

Adult zebrafish (male and female, 3–6 months old) were obtained from Guangzhou, China. All fish were maintained in a standardized housing system at 28 ℃ under a 14/10-h light/dark cycle and fed brine shrimp twice daily. Experimental procedures were conducted in compliance with the ethical guidelines approved by the Ethical Review

Committee of Xiamen university.

2.5.2. Mice

BALB/c mice (female, 6–8 weeks old, 20 ± 2 g) were purchased from Beijing Vital River Laboratory (Beijing, China). Mice were randomly housed in individually ventilated cages (IVCs) and provided with the standardized food and water. The animal rooms were maintained in standardized environmental conditions (temperature: 22 ± 2 ℃, humidity: 50 ± 10 %, a 12/12-h light/dark cycle) for one-week acclimatization period prior to experiments. To initiate the infection model, all animal procedures were strictly carried out in accordance with of Institutional Animal Care and Use Committee (IACUC) at Xiamen university under protocol (accreditation number, XMULAC20230053). On the study termination day, all mice were humanely euthanized by CO_2 for the collection of vital organs and skin tissues for analysis. The number of specimens for each animal trial was specified in the corresponding figure legend.

2.6. Antimicrobial Susceptibility assays

2.6.1. Agar disc diffusion assay

The overnight cultures of *V. parahaemolyticus* and *V. vulnificus* were prepared by picking a single colony into TSB medium and incubating at 28 ℃ with shaking at 180 rpm. The bacterial suspension was standardized to match a 0.1 McFarland turbidity and subsequently diluted 1:10 in fresh TSB medium. 100 μL aliquots of diluted suspensions (approximately 1 × 10^7 CFU/mL) were spread onto Mueller-Hinton (MHB, Oxoid, UK) agar plate using sterile glass beads to give an individual growth of cells. Subsequently, 6-mm diameter filtered discs without antibiotic were placed on each plate containing the *V. parahaemolyticus* or *V. vulnificus* as an indicator. Immediately, 20 μL of Ajapocin (1, 2 mg/mL) was randomly dispensed into the sterile filter discs. Additionally, 1 mg/mL of bovine serum albumin (BSA, Macklin, Shanghai, China) was used as a negative control and the sterile Milli-Q water served as the vehicle control. Plates were incubated overnight in a humidity chamber at 28 ℃. The next day, inhibition zones on each plate were photographed and their diameters were measured using a vernier caliper [27]. Experiments were repeated in three independent times (n = 3).

2.6.2. MIC assay

The anti-*Vibrio* activity assay of Ajapocin was evaluated using a standard broth microdilution method recommended by the Clinical and Laboratory Standard Institute (CLSI) guidelines [28]. PMB sulfate was chosen as a reference antibiotic for comparison. In short, overnight cultures of the tested strains were diluted approximately 1 × 10^6 CFU/mL in TSB medium. 50 μL aliquot of bacterial suspensions was dispensed into the each well of flat-bottom 96-well microplates. Afterwards, Ajapocin and PMB were prepared in TSB medium to make final concentrations ranging from 3 μM to 48 μM. An equal volume of each peptide or antibiotic dilution was added to the corresponding wells containing the bacterial suspensions. The cultures were incubated with sterile Milli-Q water as the vehicle control. After incubation at 28 ℃ for 18–24 h, MIC values were determined at lowest concentration of the agents at which no visible bacterial growth was appeared, based on visual inspection. All assays were repeated in three independent experiments (n = 3).

2.6.3. Time-dependent killing assay

Time-kill kinetic assays were performed as described for the above MIC assay with the following modifications [29]. Briefly, *V. parahaemolyticus* and *V. vulnificus* were grown in TSB medium until reaching an optical density $(OD)_{600}$ of 0.5. Then the bacterial cells were harvested by centrifugation, washed, and resuspended in fresh TSB medium to a density of approximately 1 × 10^6 CFU/mL. 100 μL aliquots of the bacterial suspensions were incubated with Ajapocin solutions at the final concentrations of 1 × and 2 × MIC. An equal volume of PMB (1 × MIC) and sterile Milli-Q water were served as controls. At designed time points, the mixtures were diluted 10-fold and plated onto the TSB agar plates. After statical incubation overnight at 28 ℃, bacterial colony-forming units (CFUs) were counted, and the killing efficiency was calculated based on the formula.

Bacterial viability (%) = (recovered CFUs/ initial CFUs) × 100 %

Where the initial CFUs were represented the bacterial colonies in distinct groups at 0 min, and recovered CFUs were indicated the total viable colonies at intervals. Experiments were performed in three biologically independent samples (n = 3).

2.7. Scanning and Transmission electron microscopy characterization

2.7.1. Scanning electron microscopy (SEM) Analysis

SEM was utilized to examine the morphological alternations in bacteria [30] following Ajapocin treatment, in addition, PMB served as a positive control. Briefly, the overnight cultured *V. parahaemolyticus* and *V. vulnificus* were diluted to 1 × 10^7 CFU/mL in TSB. 300 μL aliquots of the bacterial suspensions were incubated with Ajapocin (1 × MIC) or PMB (1 × MIC) for 1 h at room temperature. As a negative control, untreated bacterial suspensions were incubated with sodium phosphate buffer (NaPB, pH 7.4). After incubation, the samples were collected by centrifugation at 4000 rpm, washed twice with NaPB buffer, and the cell pellets were fixed overnight at 4 ℃ in 2.5 % glutaraldehyde (Sigma-Aldrich, USA). The following day, samples were gently washed twice with assay buffer and deposited onto polylysine-coated slides for 20 min on ice to allow adherence. Subsequently, all samples were conducted the dehydration process using a graded ethanol (SINOPHARM, China) series (30 %, 50 %, 70 %, 90 % and 95 %) at 15 min each, and 100 % ethanol solution twice for 20 min at intervals. All specimens were sequentially dried and coated, ultimately visualized using a Zeiss SUPRA 55 SEM (Zeiss, Germany).

2.7.2. Transmission election microscopy (TEM) analysis

TEM was next applied to investigate the ultrastructural alternations of bacteria [31]. Similar to SEM description, the bacteria were prepared and incubated with Ajapocin under the same conditions. After incubation for 1 h, the samples were harvested and embedded in 2 % agar blocks for 30 min at room temperature to maintain structural integrity. Moreover, the samples were fixed overnight in 2.5 % glutaraldehyde (SPI, USA) at 4 ℃. The next day, the mixtures were washed three times with NaPB buffer and post-fixed with 1 % osmium tetroxide (Sigma-Aldrich, USA) for 2 h at room temperature. After removing the osmium tetroxide solutions, the samples were gently washed with Milli-Q water, and further dehydrated in a graded ethanol (30 %, 50 %, 70 %, 90 %, 95 % and 100 %) for 15 min at intervals. Afterwards, the samples were rinsed with acetone (SINOPHARM, China), infiltrated and embedded in epoxy resin (SPI, USA). After complete resin permeabilization, ultrathin sections (50–70 nm) of specimens were cut and equipped on 3-mm copper grids. The samples were sequentially stained with uranyl acetate (SINOPHARM, China) and lead citrate (SINOPHARM, China) for 10 min. Finally, all images were obtained using a HT7800 TEM (Hitachi, Japan).

2.8. Membrane permeation assay

2.8.1. Outer-Membrane permeability assay

The outer membrane integrity was evaluated using a NPN dye [32]. In short, the overnight bacterial cultures were collected, washed and resuspended in HEPES buffer (5 mM HEPES, 5 mM glucose, pH 7.4, Sigma-Aldrich, USA). The bacterial suspensions (1 × 10^6 CFU/mL) were then pre-mixed with NPN (10 μM) for 10 min at room temperature. Afterwards, 50 μL aliquots of NPN-labelled bacterial cells were added

into a black, opaque flat-bottom microplate. Later, an equal volume of Ajapocin was added to the wells at the final concentrations of 1 × and 2 × MIC. PMB at 1 × and 2 × MIC was chosen as a positive control. After incubation for 30 min at room temperature, fluorescent intensity of each well was recorded on a Microplate Reader (Tecan, Switzerland) with the excitation/emission wavelength of 350/420 nm. Experiments were performed in three biologically independent replicates ($n = 3$).

2.8.2. Inner-Membrane integrity assay

The inner membrane perturbation assay was conducted using a LIVE/DEAD™ *Bac*light Bacterial Viability Kit [33]. Briefly, the overnight cultured *V. parahaemolyticus* and *V. vulnificus* were diluted to 1 × 10^7 CFU/mL in TSB medium. 50 μL aliquots of suspensions were incubated with equal volume of Ajapocin (1 ×, 2 × MIC) in a black, clear-bottom 96-well plate. Additionally, 1 × MIC of PMB was chosen as control. After incubation for 1 h, each well of plates was gently washed twice in phosphate-buffered saline (PBS) and mixed with SYTO 9 (1.67 μM) and PI (10 μM) dyes according to manufacturer's instruction. After incubation for additional 15 min in the dark, fluorescence images of stained cells were examined using the confocal laser scanning microscopy (CLSM) under a 100 × oil immersion objective (Zeiss, Germany).

2.8.3. Cytoplasmic membrane depolarization assay

The membrane depolarization effects were evaluated using a fluorescent probe $DiSC_3(5)$ [34]. Briefly, the overnight cultures were harvested and resuspended in HEPES buffer. The cell suspensions (1 × 10^6 CFU/mL) were pre-mixed with $DiSC_3(5)$ at 0.5 μM for 10 min in the dark. After incubation, 50 μL of stained samples were added into each well of black, opaque flat-bottom plates. Immediately, the initial fluorescent intensity was determined using a Microplate Reader (Ex = 620 nm, Em = 670 nm) at 2-min intervals for 10 min. Afterwards, 50 μL aliquot of Ajapocin (1 ×, 2 × MIC) was transferred into plates. In addition, PMB (1 ×, 2 × MIC) was chosen as the positive control as well sterile water was used as the vehicle control. The fluorescence intensity was measured using a Microplate Reader (Ex = 620 nm, Em = 670 nm) at 2-min intervals for additional 30 min. Curves were plotted by GraphPad Prism10. Experiments were performed in three biologically independent samples ($n = 3$).

2.9. Bacterial lysis assay

Bacterial viability assays were conducted on *V. parahaemolyticus* and *V. vulnificus* by evaluating PI-uptake activity [35]. In short, the overnight cultures of bacteria were diluted to 1 × 10^7 CFU/mL in TSB medium. 200 μL aliquots of bacterial suspensions were then incubated with equal volume of Ajapocin at corresponding 1 × and 2 × MIC for 30 min. PMB (1 ×, 2 × MIC) was chosen as the positive control, and equal volume of assay buffer was used as a negative set. Subsequently, all mixtures were washed twice in PBS buffer and mixed with PI (10 μM) for 15 min in the dark. After incubation, samples were immediately operated using the flow cytometry (Beckman, USA) with excitation wavelength at 535 nm and emission wavelength at 615 nm. The proportion of PI-labeled cells was quantified using CytExpert software.

2.10. LPS and phospholipid Competitive assay

The antimicrobial activity between Ajapocin and membrane compounds was determined using both agar diffusion assay and chequerboard microdilution assay [33,36]. In disc diffusion assay, 50 μL of Ajapocin (1 mg/mL) was pre-mixed with equal volume of LPS (1 mg/mL) or CL (1 mg/mL) for 30 min. After incubation, 20 μL of Ajapocin-LPS mixture and Ajapocin-CL mixture were dropped into the filter paper discs of MH agar plates containing *V. parahaemolyticus* (2 × 10^6 CFU/mL) or *V. vulnificus* (2 × 10^6 CFU/mL), respectively. The plates were incubated overnight at 28 ℃. The next day, inhibition zones of plates were photographed and measured on the basis of agar diffusion assay. In chequerboard microdilution assay, peptide Ajapocin was serially diluted in TSB medium ranging from 6 μM to 96 μM. 50 μL of this dilution was added along the abscissa in a flat-bottom 96-well plate. Moreover, same volume of bacterial suspensions (1 × 10^6 CFU/mL) were added along the ordinate containing LPS, CL or PC at concentrations ranging from 2 μM to 128 μM. In addition, PMB was used as the positive control in LPS supplement assay. Assay plates were incubated overnight without shaking, determination of MICs was referred to MIC assay. The fold change in MIC of Ajapocin was plotted using GraphPad Prism 10.0.

2.11. Confocal microscopy of localization analysis

The overnight cultures of *V. parahaemolyticus* and *V. vulnificus* bacteria were prepared according to bacterial lysis assay. To demonstrate Ajapocin's subcellular localization [37] on each strain, 50 μL aliquots of bacterial suspensions (1 × 10^7 CFU/mL) were transferred into the black, clear-bottom 96-well plate, then, each well of plate was incubated with equal volume of FITC-Ajapocin at final concentrations of 1 × and 2 × MIC, respectively. Bacterial cultures treating with sterile water instead of peptide were served as controls. After incubation for 1 h at 28 ℃ in the dark, the supernatants were gently aspirated and supplemented with 50 μL of assay buffer containing DAPI dye (10 μM). Samples were stained for additional 15 min in the dark. Finally, images of samples were examined using the CLSM under a 63 × oil immersion objective.

2.12. Cytotoxicity test

Ajapocin's toxicity assay was assessed using a cell counting kit-8 (CCK-8, Lablead, Beijing, China) method with minor modifications [38]. In short, both ZF 4 cells (1 × 10^5 cells/mL) and HaCaT cells (1 × 10^5 cells/mL) were seeded in 96-well plates. The cells were then cultivated overnight at corresponding temperatures with a humidified atmosphere of 5 % CO_2. Thereafter, Ajapocin peptide was serially diluted into each well of the plates at final concentrations ranging from 4 μM to 32 μM. Cells were incubated with Melittin (24 μM) and sterile Milli-Q water without peptide as control. At 24, 48 and 72 h, the mixtures were removed the spent medium, washed with Hanks' balanced salt solution (HBSS) buffer, and replaced with freshly prepared complete medium containing CCK-8 reagent according to manufacturer's instructions. Under additional 2 h incubation in the dark, the absorbance of samples at 490 nm was measured using a Microplate Reader. Cell viability was calculated using the following formula.

Cell viability (%) = $[(OD_{Ajapocin} - OD_{blank}) / (OD_{control} - OD_{blank})] \times 100$ %.

Experiments were performed in three biologically independent samples ($n = 3$).

2.13. Toxicity evaluation in vivo

The *in vivo* toxicity evaluation was conducted referred on previous reported method with slight modification [39]. In short, female BALB/c mice (6–8 weeks old) were purchased from Beijing Vital River. Mice were divided into three groups randomly and accepted different treatments: Ajapocin-treated cohort ($n = 4$ mice) was injected intraperitoneally with a single dose of 5 mg/kg, both PMB-treated cohort (5 mg/kg) and saline-treated cohort were used as the controls ($n = 4$ mice per group). Animals were injected daily for a week to monitor for adverse effects and mortality once a day, and body weights and animal behaviors were also recorded. After normal feeding for days 8, prior to the euthunization, blood was collected for serum biochemical analysis, including alanine aminotransferase (ALT), aspartate aminotransferase (AST), urea nitrogen (BUN) and creatinine (CRE). Organs such as kidney and liver were harvested for histological analysis via standard hematoxylin and eosin (H&E) staining.

2.14. Zebrafish-Vibrio infection model

The investigation of Ajapocin's activity on zebrafish infection model was conducted according to previously reported [40,41]. In brief, zebrafish ($n = 20$ fish per group) were randomly divided into a control and three experimental groups for preparation. Based on the pre-experimental data, we opted the lethal density of *V. parahaemolyticus* (5×10^7 CFU/mL) and *V. vulnificus* (2.5×10^7 CFU/mL) for use. The overnight cultured bacteria were washed twice and resuspended in PBS buffer. Later, each fish of experimental groups was intraperitoneally injected with 8.8 μL of bacterial suspension using a Hamilton device (Hamilton, Reno, USA). The control group were injected with 8.8 μL of assay buffer. At 2 h post infection, Experimental zebrafish were challenged with 8.8 μL of saline, Ajapocin (1 mg/mL) and PMB (1 mg/mL) via intraperitoneal administration. At 6, 12, 24 and 36 h post infection, we monitored the survival rate of zebrafish during treatment period. Upon plotting survival curves, *P* values were calculated using a log-rank (Mantel-Cox) test.

2.15. Mice Full-Thickness wound infection model

To establish a *V. vulnificus*-infected full thickness model [31,42], 6- to 8-week-old female BALB/c mice were husbandary before day −7 infection. On Day 0, the overnight cultures of *V. vulnificus* were harvested and resuspended in PBS buffer for use. Their hairs were removed from the anesthetized mice, later, the dorsal skin of mice was established two full-layer excisional wounds with 7-mm diameter using a skin biopsy punch. 10 μL aliquots of bacterial suspension (1×10^8 CFU/mL) were inoculated into the two wounds, which were left to settle for 2 h and allowed the inoculated bacteria to cause infections. Subsequently, the mice were randomly divided into following three groups ($n = 4$ mice per group) and treated with distinct solutions: saline, Ajapocin (1 mg/mL, 10 μL) and PMB (1 mg/mL, 10 μL) group, which was administered for 3 times at 0, 1 and 2 days before covering the infected wounds with the 3 M Transparent Tegaderm Patch (Minnesota, USA). Additionally, the wounds were photographed before peptide/antibiotic administration and on days 0, 3, 5, 8 and 12 of treatment period. At 12 days, all mice were humanely euthanized, immediately, the excised wound tissues with 5-mm of peripheral region were homogenized in TSB medium, and the samples were serially diluted in TSB medium. Afterwards, samples were spread onto the TSB agar plates. After incubation overnight at 28 ℃, bacterial colonies were counted and quantified in each wound. In addition, wound areas were measured using the ImageJ and relative wound area was calculated on the basis of the following equation: relative wound area = wound area at certain day/wound area on day 0. The pathological analysis of representative wound tissues was evaluated via both H&E staining and Masson's trichrome staining.

2.16. Statistics and Reproducibility

Experiments were replicated and repeated, and data are presented as mean ± standard deviation (SD). MICs were defined as the lowest concentrations that fully inhibited the growth of pathogens. Zebrafish-*Vibrio* infection assays were analyzed using Kaplan-Meier survival curves, and *P* values calculated via the log-rank (Mantel-Cox) test. For multiple comparisons at a single time point, data were analyzed using one-way analysis of variance (ANOVA). For data obtained at multiple time points, two-way ANOVA was utilized. Appropriate post *hoc* tests (e.g., Dunnett's, Tukey's) were performed to correct for multiple comparisons, with specific details provided in the respective figure legends. Asterisks ($^*P < 0.05$, $^{**}P < 0.01$, $^{***}P < 0.001$ and $^{****}P < 0.0001$) indicate significant differences. Precise *P*-values are reported for the Zebrafish-*Vibrio* infection trials, and n.s. represents no significance. All statistical analyses were performed using GraphPad Prism 10 software. Images from SEM, TEM or CLSM are representative examples from at least three independent replicates.

Table 1
Physical-chemical properties of Ajapocin.

Physicochemical parameters	Ajapocin
Amino acid sequence	GFRIAFKRILTCGKK
Molecular weight (kDa)	1.738
Theoretical pI	11.11
Total net charge	+5
Hydrophobicity	40 %

3. Results

3.1. Antimicrobial activity of Ajapocin in vitro

To combat infections caused by *V. parahaemolyticus* and *V. vulnificus* pathogens, our study identified a novel AMP termed Ajapocin and further determined its well-defined scaffold, including beneficial physical–chemical property and typical α-helical features (Fig. 1A-**B** and Tab. 1). To demonstrate the vibriocidal effects *in vitro*, the antimicrobial activity of Ajapocin on *Vibrio* bacteria was tested by inhibition zone method. As shown in Fig. 1C and Tab. 2, at 1 mg/mL, Ajapocin exhibited potent antibacterial activity against *V. parahaemolyticus* and *V. vulnificus*, as evidenced by median inhibition zones diameters of 19.03 mm and 12.73 mm, respectively. Upon treatment with 2 mg/mL, Ajapocin displayed its more superior performance against each bacterium, resulting in significant increase in diameter with 19.96 mm and 14.15 mm. Hence, this result revealed that Ajapocin exhibited powerful activity against pathogenic *Vibrio*. Next, we continued to evaluate Ajapocin's potency using a MIC method, as shown in Tab. 3, Ajapocin displayed excellent bactericidal effect in both *V. parahaemolyticus* and *V. vulnificus* bacteria, with the MIC values ranging from 6 μM to 12 μM. In addition, we opted both AMP Spgillcin$_{177\text{-}189}$ and antibiotic PMB for comparison. Notably, Ajapocin, parallel to drug PMB but over marine-sourced Spgillcin$_{177\text{-}189}$, displayed potent activity in the killing of *V. parahaemolyticus* and *V. vulnificus*.

Next, we evaluated the bactericidal efficiency of Ajapocin on *V. parahaemolyticus* and *V. vulnificus*. As shown in Fig. 1D, results revealed that Ajapocin displayed fast-acting bactericidal ability in a dose-dependent manner. For example, at 2 × MIC, Ajapocin could respectively kill over 99.9 % of *V. parahaemolyticus* and *V. vulnificus* pathogens within 30 min and 60 min, similar to the effects of PMB treatment that rapidly eliminated both strains within 10 min and 60 min. Collectively, these results concluded that Ajapocin could have capable of treating *Vibrio* spp. infections *in vitro*.

3.2. Ajapocin Killed the Vibrio pathogens by Permeabilizing bacterial membrane

Given that superior anti-*Vibrio* activity against *V. parahaemolyticus* and *V. vulnificus*, we were encouraged to uncover the mechanism of action of Ajapocin on each bacterium. As depicted in Fig. 2A, upon SEM observation, bacterial morphology was normal and their membranes were intact in the absence of Ajapocin. Conversely, Ajapocin-treated bacteria showed morphological alternations and fragmentations, such as PMB treatment. Similarly, based on TEM analysis (Fig. 2B), we found that bacterial cells showed well-defined borders and coupled with abundant contents in the control group. In sharp contrast, Ajapocin treatment resulted in substantial permeation on bacterial membranes and subsequent leakage of intracellular content. This effect was mirrored to the PMB drug that employed its membrane-disruptive pattern to combat against Gram-negative bacteria.

We next investigated Ajapocin's molecular mechanisms in membrane permeability. Gram-negative bacteria are clad with an additional outer membrane over Gram-positive cells responsible for difficult-to-treat bacterial infection [43]. As such, we tested bacterial outer membrane permeabilization on *V. parahaemolyticus* and *V. vulnificus*. In

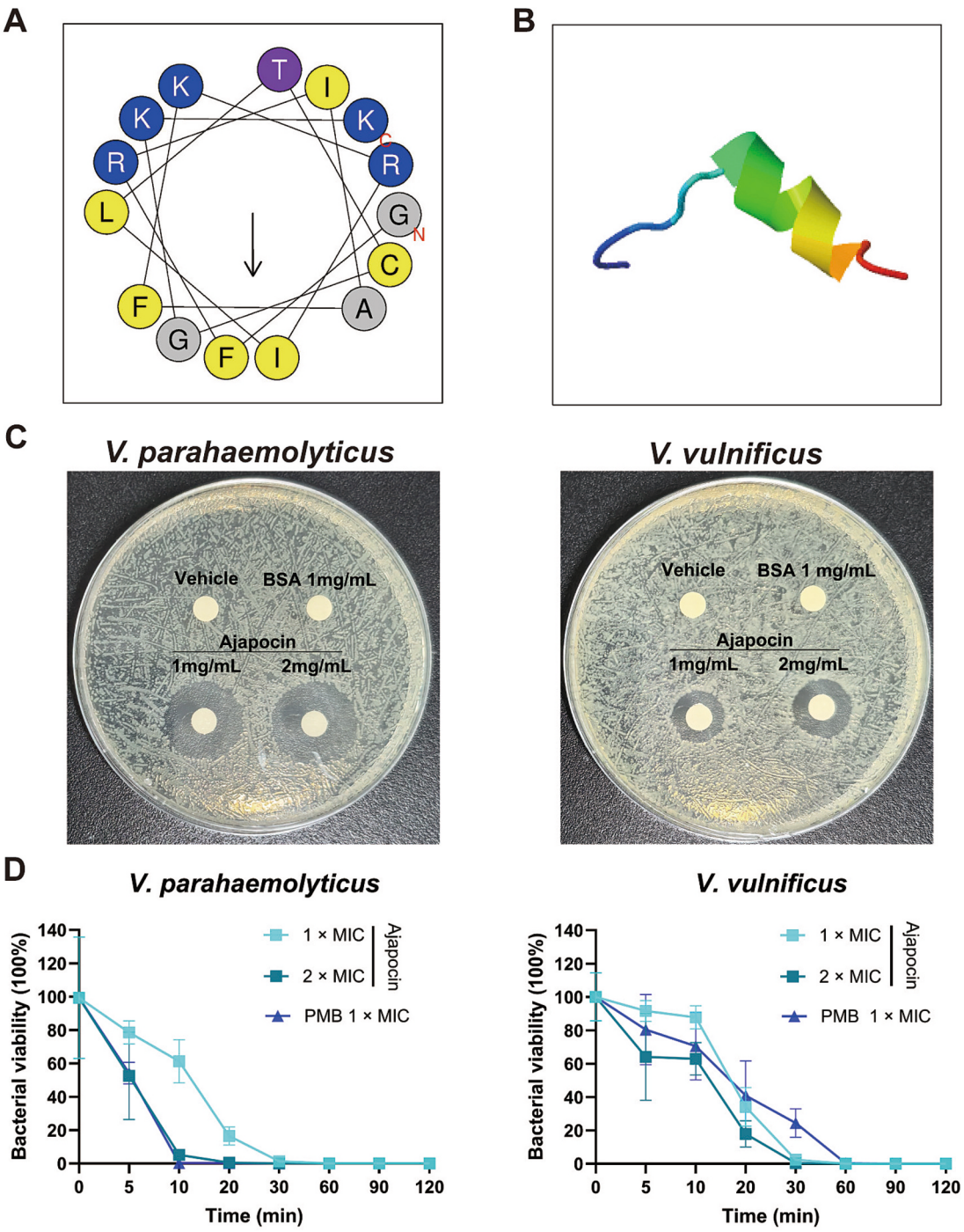

Fig. 1. Ajapocin characterization, and activity against *V. parahaemolyticus* and *V. vulnificus* bacteria *in vitro*. (A) Sequence information was analyzed using HeliQuest ((http://heliquest.ipmc. cnrs.fr/). Positively charged amino acids were shown in blue, and hydrophobic ones were shown in yellow. (B) Three-dimensional structure of Ajapocin. I-TASSER (http://zhanglab.ccmb.med.umich.edu/I-TASSER/) was used to predict the structural model. (C) Representative photographs of Ajapocin's activity against *V. parahaemolyticus* and *V. vulnificus* bacteria. (D) Time-killing kinetics of Ajapocin on *V. parahaemolyticus* and *V. vulnificus* pathogens, PMB (1 × MIC) served as the positive control. The number of viable bacteria was calculated by CFU counting. $n = 3$ biologically independent replicates.

Table 2
Anti-*Vibrio* activity for Ajapocin.

Microorganisms	**Size of Diameter (mm)***	
	Ajapocin (1 mg/mL)	Ajapocin (2 mg/mL)
V. parahaemolyticus	19.03	19.96
V. vulnificus	12.73	14.15

*Measurement of inhibition zone diameters by agar disc diffusion assay. Data were represented median values of three biologically independent replicates.

Table 3
The MIC of Ajapocin against *V. parahaemolyticus* and *V. vulnificus*.

Antimicrobials	**Bacteria**	
	V. parahaemolyticus	*V. vulnificus*
Ajapocin	6 μM	12 μM
$Spgillcin_{177\text{-}189}$	12 μM	> 24 μM
PMB	6 μM	12 μM

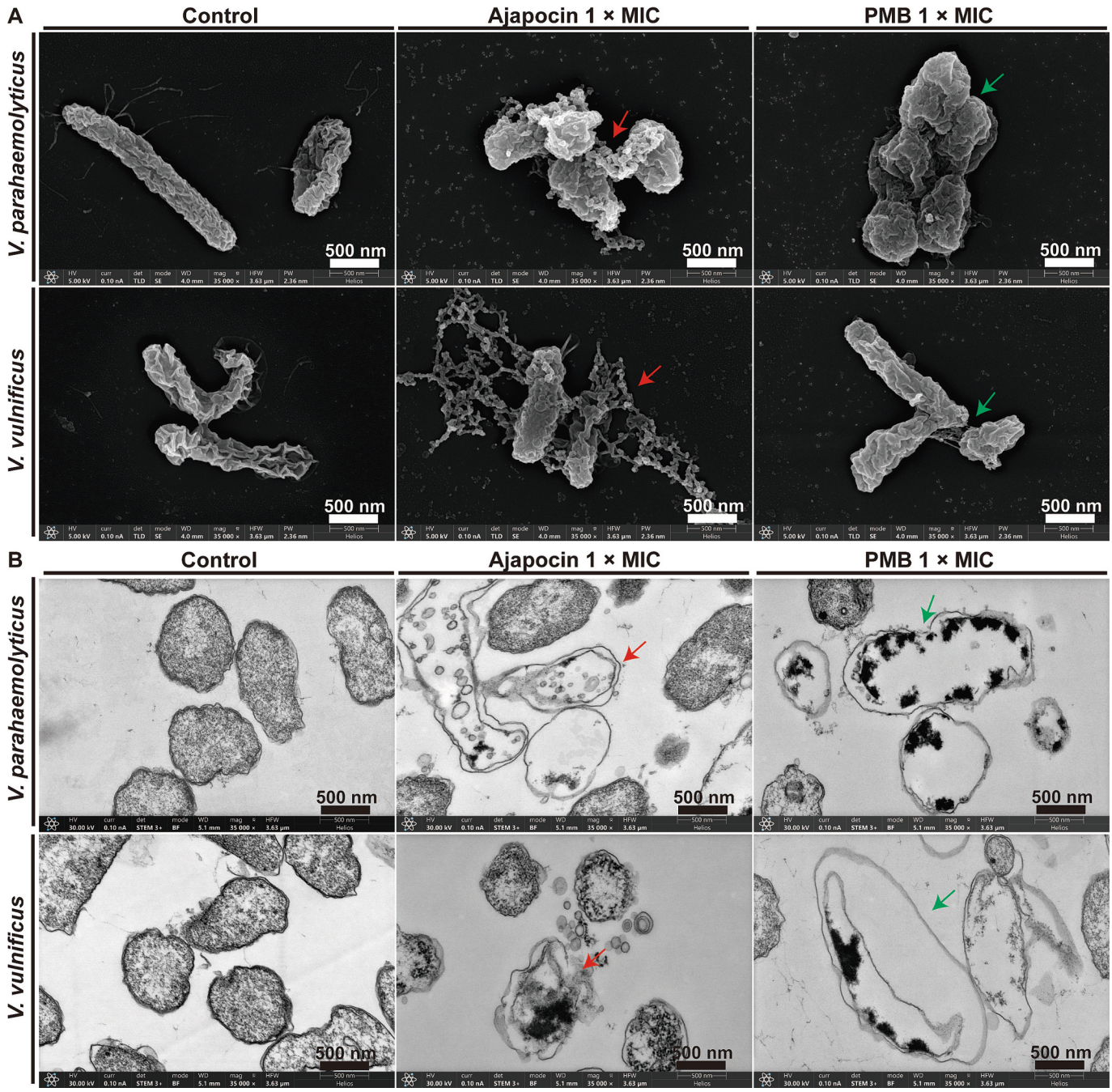

Fig. 2. Mechanism of action of Ajapocin on bacterial membrane disruption. (A) SEM images of *V. parahaemolyticus* and *V. vulnificus* bacteria treated with Ajapocin (1 × MIC). PMB (1 × MIC) was used as the positive control. Scale bars, 500 nm. (B) TEM images of *V. parahaemolyticus* and *V. vulnificus* bacteria treated with Ajapocin (1 × MIC). PMB (1 × MIC) was used as the positive control. Scale bars, 500 nm.

comparison to control bacteria (Fig. 3A), following treatment with Ajapocin at 2 × MIC, Ajapocin ($P < 0.001$) exhibited intense outer membrane disruption in *V. parahaemolyticus*, as evidenced by around 1.3-fold increase in fluorescence intensity. Similarly, compared to untreated bacteria, Ajapocin treatment ($P < 0.0001$) remarkedly altered outer-membrane permeability against *V. vulnificus*, resulting in significant increase in fluorescence intensity for 1.4-fold values. This result indicated that Ajapocin altered the membrane permeation against pathogens. Moreover, we continued to examine the inner membrane variation of aforementioned bacteria (Fig. 3B). We found that no observable PI signals in control group. However, Ajapocin treatment resulted in clear and intense PI fluorescence signals in both pathogenic bacteria. Notably, PMB exhibited weak activity against *V. vulnificus* (Fig. 3C), displaying a significant SYTO 9 signal in a single cell. However, the PI signal was also obviously detected following Ajapocin treatment at 2 × MIC. Therefore, Ajapocin could induce membrane damage by altering both outer and inner membrane permeation on tested *Vibrio* bacteria.

Herein, we assessed the membrane depolarization using a membrane potential indicator, $DiSC_3(5)$ dye. As shown in Fig. 3D, compared to control, Ajapocin substantially dissipated membrane potential of both *V. parahaemolyticus* and *V. vulnificus*, echoing the above conclusion by Ajapocin-membrane interaction. Strikingly, Ajapocin showed superior activity to PMB. These observations implied that Ajapocin might manifest the discriminate advantage in membranolytic mechanism against *Vibrio* pathogens.

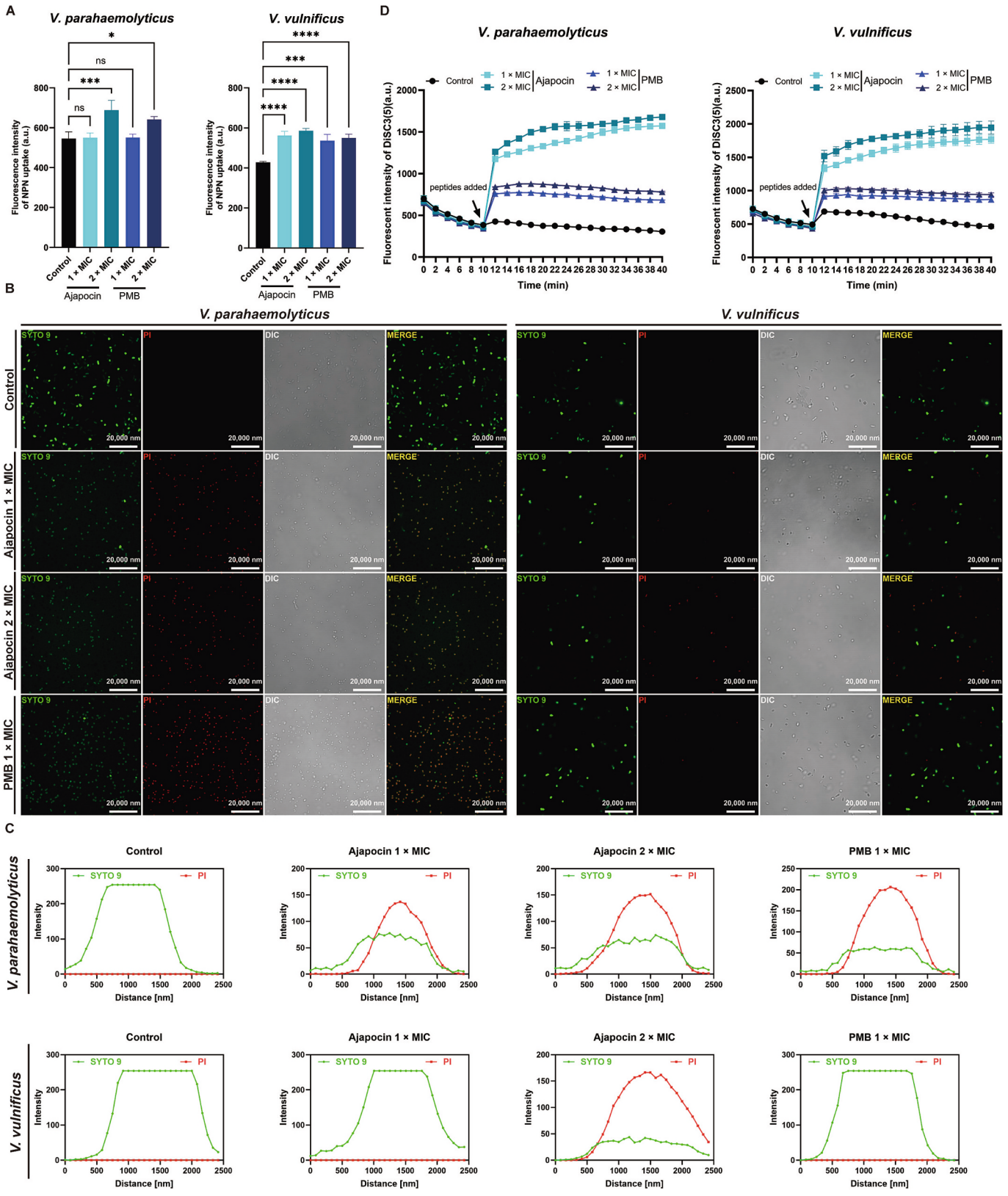

Fig. 3. Ajapocin caused bacterial damage in membrane permeation patterns. (A) Outer-membrane permeability of *V. parahaemolyticus* and *V. vulnificus* pathogens treated with Ajapocin (1 ×, 2 × MIC), as monitored by NPN fluorescent values. PMB (1 ×, 2 × MIC) was used as control. $n = 3$ biologically independent replicates. Statistical analysis was evaluated using the Dunnett's test compared to control: $^{*}P < 0.05$, $^{***}P < 0.001$ and $^{****}P < 0.0001$. n.s. represented no significance. (B) Inner-membrane integrity of *V. parahaemolyticus* and *V. vulnificus* pathogens treated with Ajapocin (1 ×, 2 × MIC), as assessed by SYTO 9 and PI staining. PMB (1 × MIC) served as control. Scale bars, 20,000 nm. (C) Both SYTO 9 and PI of fluorescence disruption curves in the single-cell region of B for *V. parahaemolyticus* and *V. vulnificus* bacteria. (D) Cytoplastic membrane depolarization of *V. parahaemolyticus* and *V. vulnificus* pathogens treated with Ajapocin (1 ×, 2 × MIC), as monitored by $DiSC_3(5)$ values. PMB treatment (1 ×, 2 × MIC) was used as control. $n = 3$ biologically independent replicates.

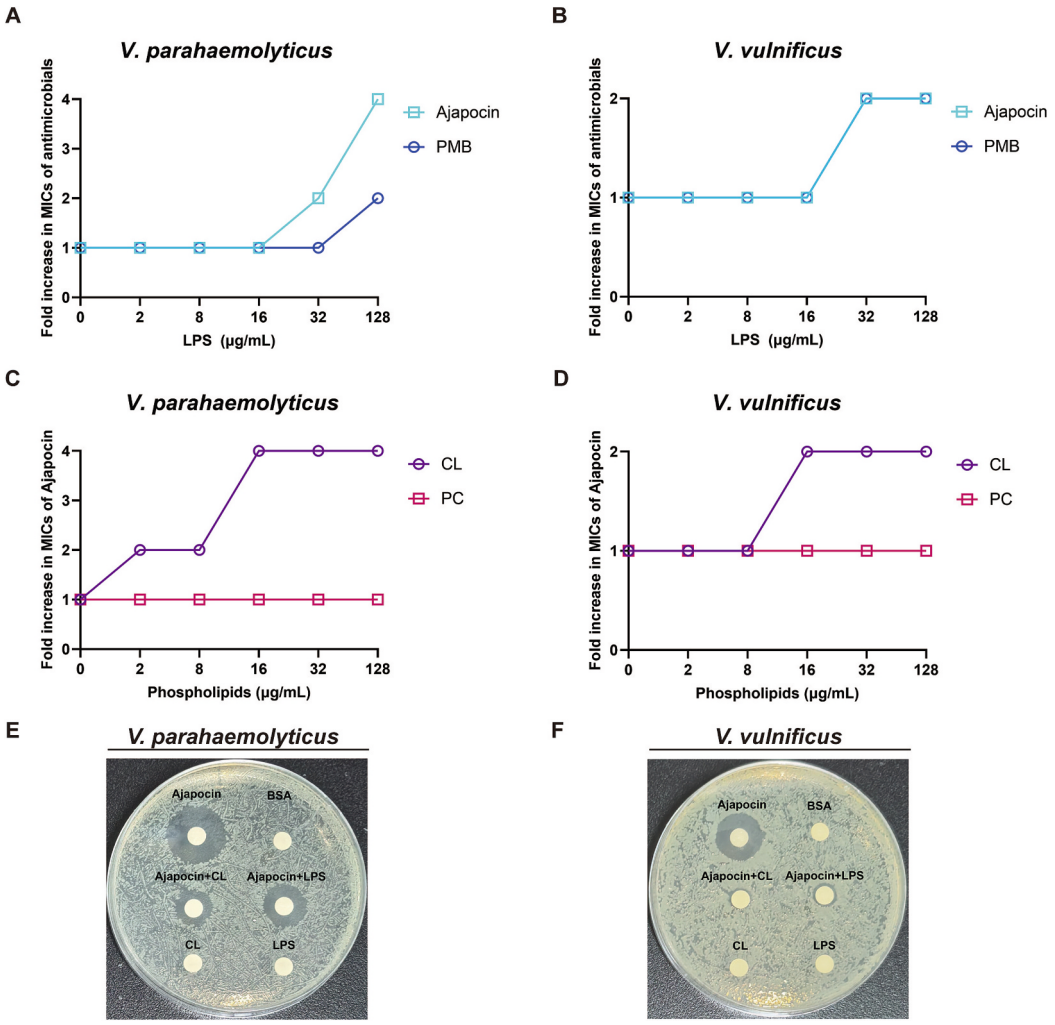

Fig. 4. Ajapocin showed membrane-interacting profiles by targeting membrane components. (A, B) Fold increase in MIC of Ajapocin on *V. parahaemolyticus* and *V. vulnificus* at exogenous addition of LPS (2–128 μM). PMB was used as control. (C, D) Fold increase in MIC of Ajapocin against *V. parahaemolyticus* and *V. vulnificus* at exogenous addition of CL (2–128 μM) and PC (2–128 μM). (E, F) Schematic of bactericidal assay of Ajapocin (1 mg/mL) against *V. parahaemolyticus* and *V. vulnificus* in the presence of LPS (1 mg/mL) and CL (1 mg/mL).

Table 4
Bactericidal activity of Ajapocin at addition of LPS or CL.

Antimicrobials	Size of Diameter (mm)*	
	V. parahaemolyticus	*V. vulnificus*
Ajapocin	19.39	17.10
Ajapocin + LPS	14.12	7.92
Ajapocin + CL	11.70	7.24

*Measurement of inhibition zone diameters by agar disc diffusion assay. Data were represented median values of three biologically independent replicates.

3.3. Ajapocin displayed membrane-targeting and Membrane-penetrating mechanism

To shine light on peptide-membrane interactions and gain an insight into the potential target, we first analyzed the interaction between Ajapocin and LPS, an abundant component in Gram-negative bacteria. As shown in Fig. 4**A-B**, we found that Ajapocin attenuated its bacterial activity against both *V. parahaemolyticus* and *V. vulnificus* at exogenous addition of LPS, uncovering the intrinsic mechanism similar to the LPS-targeting PMB. Hence, Ajapocin acted as a cell envelope-acting peptide on *Vibrio* pathogens. We continued to evaluate the antibacterial activity in the presence of phospholipids, including CL of bacterial components [44] and PC of mammalian cells [45]. As shown in Fig. 4**C-D**, our results demonstrated that CL, but not PC, impaired Ajapocin's anti-*Vibrio* activity in the killing of *V. parahaemolyticus* and *V. vulnificus*. Thus, we demonstrated that positively charged Ajapocin could interact with negatively charged membranes by targeting LPS and CL in bacterial surface. We also noted that Ajapocin maintained its bactericidal activities at addition of PC components, confirming the precise mechanism via electronic interaction, and suggesting that Ajapocin's favorable biocompatibility. We validated potential targets of Ajapocin against *Vibrio* bacteria, as shown in Fig. 4**E-F** and Tab. 4. We found both LPS and CL substantially abolished Ajapocin's activity against *Vibrio* strains. Collectively, we unveiled unique mechanisms of multi-targets implicated in binding both LPS and CL of bacterial membrane.

To address the deeper molecular mechanism of Ajapocin on *Vibrio* bacteria, we introduced FITC-Ajapocin to determine the subcellular localization. As shown in Fig. 5**A-B**, pathogenic bacteria were stained with DAPI exclusively in the control group. However, following treatment with green fluorescent-labeled Ajapocin, we observed that bacterial cells were enriched intense green signals, strikingly, their nuclear signals overlapped with the peptide signal. Thus, these results demonstrated that Ajapocin could cross cytomembrane and penetrate into bacteria. For live/dead bacterial cell discrimination, we recorded bacterial death using a PI-influx method. As shown in Fig. 5C, majority class

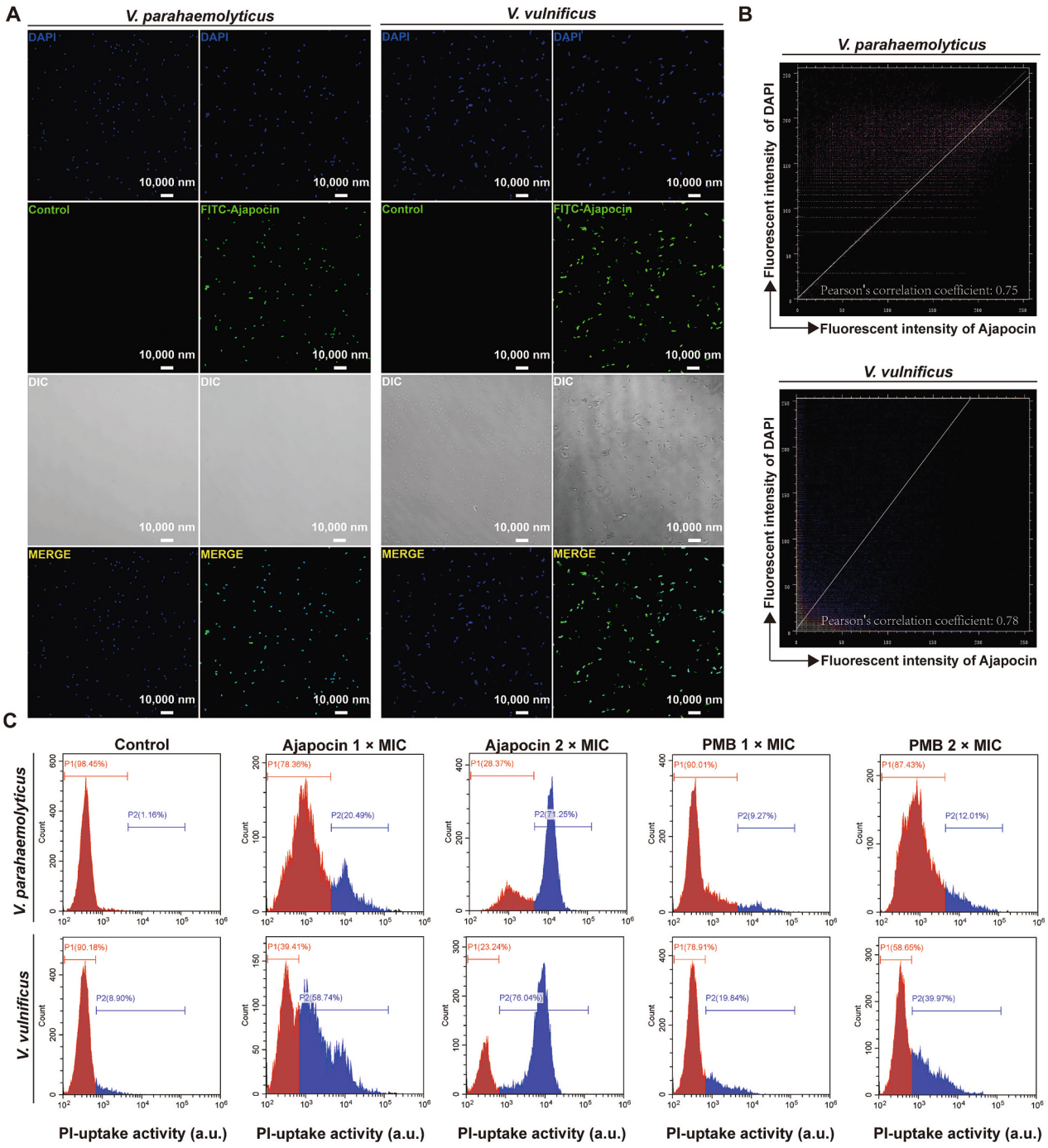

Fig. 5. Ajapocin penetrated into bacteria and induced bacterial death. (A) Immunofluorescence staining images of *V. parahaemolyticus* and *V. vulnificus* treated with FITC-Ajapocin. Scale bars, 10,000 nm. (B) Representative histograms of two-dimensional fluorescence intensity of stained bacteria. The co-localization between DAPI and FITC-Ajapocin in bacterial cells was determined using Pearson's correlation coefficient. (C) PI-uptake activity of *V. parahaemolyticus* and *V. vulnificus* bacteria treated with Ajapocin ((1 ×, 2 × MIC), as measured by PI values. PMB (1 ×, 2 × MIC) was used as the control.

were viable bacteria in untreated group, but Ajapocin treatment facilitated to kill both bacteria. Such as Ajapocin at 2 × MIC, which resulted in the large amounts of apoptotic bacteria of *V. parahaemolyticus* (71.25 %) and *V. vulnificus* (76.04 %), respectively. Moreover, at the same dosage of 2 × MIC, Ajapocin showed potency better than PMB that contributed to enhance the PI-uptake activity on both *V. parahaemolyticus* (12.01 %) and *V. vulnificus* (39.97 %) bacteria. These data collectively elucidated Ajapocin employed its unique membrane-disruptive mechanisms to combat against *V. parahaemolyticus* and *V. vulnificus* pathogens.

3.4. Ajapocin had no toxicity in vitro and in vivo

Safety is necessary for antimicrobials candidacy to advance into clinical trials, in particular with Melittin and PMB exhibiting robust potency and high toxic profiles [46,47]. Thus, we evaluated Ajapocin's potential toxicity both *in vitro* and *in vivo*. We first developed cytotoxic evaluation using ZF4 and HaCaT cell lines. As shown in Fig. 6A, compared to control, we found that Ajapocin did not affect the cellular viability on both ZF4 cells and HaCaT cells in a time- and concentration-independent manner. In sharp contrast, Melittin at 24 μM exhibited significant killing activity. This result demonstrated that Ajapocin had

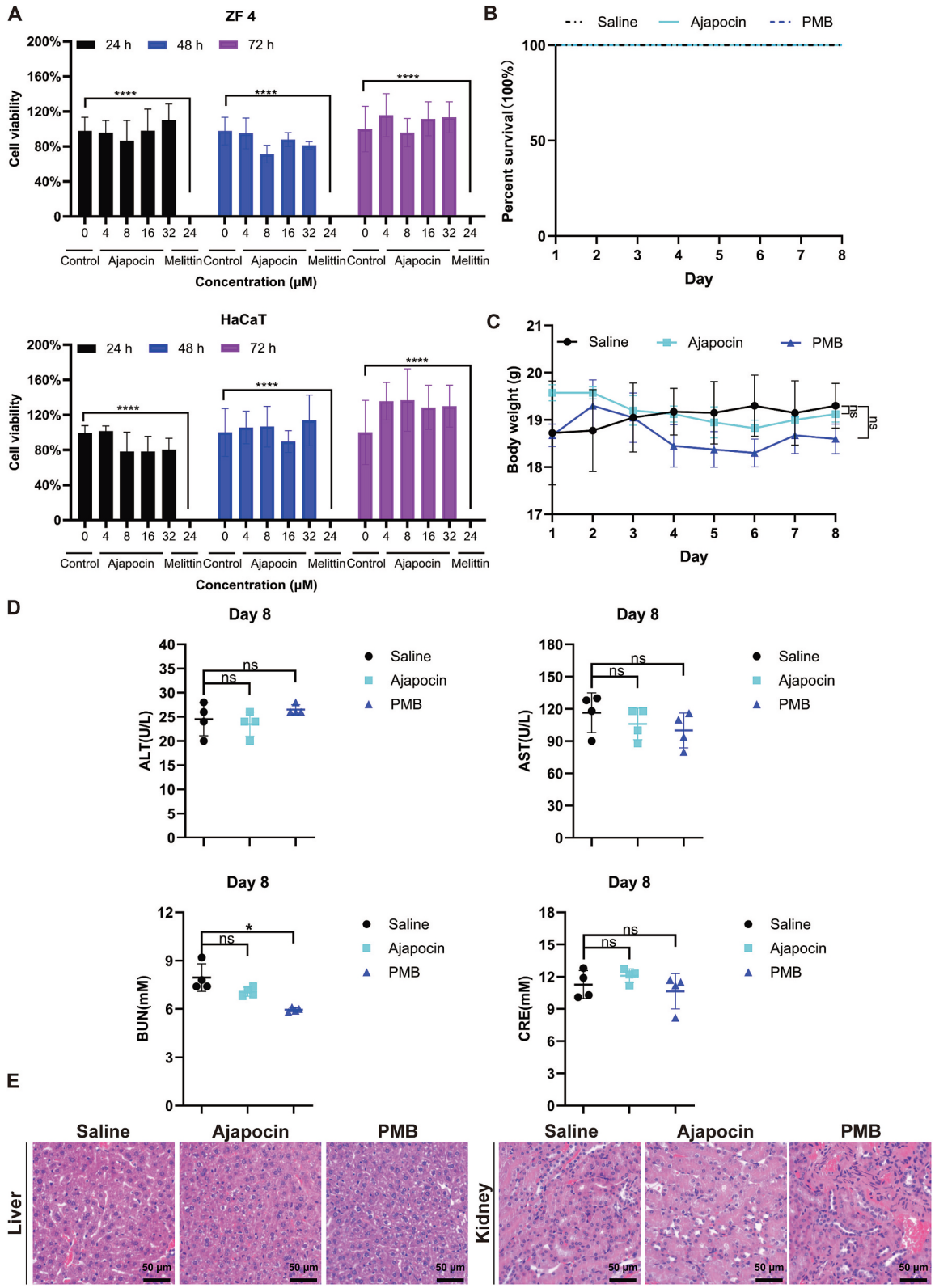

Fig. 6. Ajapocin toxicity *in vitro* and *in vivo*. (A) Toxic effects of cell lines (ZF 4 and HaCaT cells) treated with Ajapocin (4–32 μM). Melittin (24 μM) was used as the positive group. $n = 3$ biologically independent replicates. Statistical analysis was conducted using the Dunnett's test compared to control: $^{****}P < 0.0001$. (B) Survival rate of mice was monitored during the 8-day experimental period. $n = 4$ biologically independent animals. (C) Body weight of mice was monitored during the 8-day experimental period. $n = 4$ biologically independent animals. Statistical analysis was conducted using the Dunnett's test compared to saline group. n.s. represented no significance. (D) Serum biochemical indices (ALT, AST, BUN and CRE) on day 8 following a 7-day saline, Ajapocin (cumulative dose: 35 mg/kg) or PMB (cumulative dose: 35 mg/kg) treatment regimen. $n = 4$ biologically independent samples. Statistical analysis was conducted using the Dunnett's test compared to saline group: $^{*}P < 0.05$. ns represented no significance. (E) Representative images of liver and kidney sections after treatment with saline, Ajapocin and PMB via H&E staining. Scale bars, 50 μm.

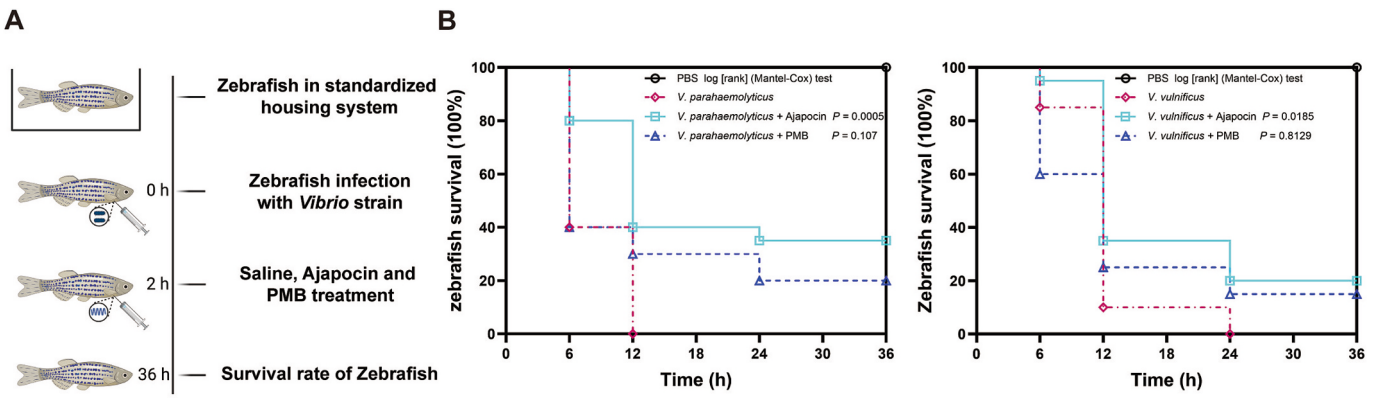

Fig. 7. Ajapocin improved the survival rate of zebrafish after *Vibrio* infection. (A) Schematic depiction of the establishment of zebrafish infection and treatment experiments. (B) Survival rate of zebrafish. zebrafish ($n = 20$ fish per group) were infected with *V. parahaemolyticus or V. vulnificus* via intraperitoneal injection. At 2 h post infection, zebrafish was intraperitoneally injected with a single dose of Ajapocin and PMB. As the vehicle group, zebrafish was intraperitoneally injected with a single dose of PBS buffer. *P* values were determined using the two-sided, log[rank] (Mantel-Cox) methods.

not been shown noticeable cytotoxic activity towards two normal cells. Next, we assessed the cumulative toxicity of Ajapocin in mice. As depicted in Fig. 6B-**C**, after a daily intraperitoneal injection for 1 week at the cumulative doses (35 mg/kg), Ajapocin retained a 100 % survival rate in mice. Meantime, we did not observe the statistical difference in body weight compared to saline-treated group. To further evaluate the potential toxicity *in vivo*, we examined the liver chemistry profiles (Fig. 6D), similar levels of serum AST and ALT indicated a lack of liver toxicity. In addition, kidney profile analysis revealed no significant change in serum BUN and CRE between saline- and Ajapocin-treated group, demonstrated no acute toxicity to kidney. Moreover, upon Ajapocin treatment, both liver and kidney organs retained normal morphology via histological examination (Fig. 6E), evidencing no structural changes and inflammatory infiltration. However, administration of PMB showed renal toxicity compared to vehicle group, leading to a marked decrease in BUN levels and accompanied by obvious inflammatory infiltration in renal pathological section. Taken together, Ajapocin failed to display toxic effects *in vitro* cellular assay and *in vivo* animal model.

3.5. Efficacy evaluation of infected zebrafish and mice wound model

Given that Ajapocin's superior antimicrobial performance on *Vibrio* pathogens *in vitro*, we continued to comprehensively investigate the therapeutic efficacy *in vivo*. First, we established a zebrafish infection model challenged with *V. parahaemolyticus* and monitored the survival rate of zebrafish during 36 h postinfection period. As shown in Fig. 7A-B, after 2 h infection of *V. parahaemolyticus* at a lethal concentration (5×10^7 CFU/mL), zebrafish of PBS-treated group was all died within 12 h. However, the Ajapocin-treated zebrafish ($P < 0.001$) strikingly increased the survival rate, rescuing 35 % at 36 h. To confirm this efficacy, we subsequently developed a zebrafish infection model caused by *V. vulnificus* bacteria (2.5×10^7 CFU/mL). Similarly, in the PBS group, 100 % of zebrafish were died at 24 h post infection, conversely, Ajapocin treatment ($P < 0.05$) showed effectiveness on protecting infected zebrafish from death, demonstrating 20 % of survival rate for 36 h. Interestingly, to combat *Vibrio* infection in zebrafish model, antibiotic PMB ($P > 0.05$) failed to effectively improve the outcome in the infected zebrafish, manifesting the 20 % and 15 % of survival rate of zebrafish, respectively. Therefore, Ajapocin exhibited its potent efficacy in treating *Vibrio* pathogens.

As known, *V. vulnificus* bacteria belonged to one of opportunistic pathogens, leading to a variety of human diseases, such as skin infection. Thus, we evaluated the *in vivo* efficacy of Ajapocin in a *V. vulnificus*-infected full thickness model. This model mimicked common *V. vulnificus* infection in human, meantime, which was frequently required antibiotic therapy. As illustrated in Fig. 8A-**D**, the sequential administration of Ajapocin ($P < 0.0001$) resulted in an around 0.9-log reduction in CFU compared to saline group, showcasing the similarly effective as the PMB with not statistically significant, although PMB ($P < 0.0001$) showed an even more impressive reduction in bacterial burden for 1.5-log CFU compared with the saline group. We concluded from this experiment that Ajapocin was available for treating *V. vulnificus* infection in skin wound model. Significantly, we found that Ajapocin ($P < 0.01$) treatment substantially promoted the wound closure in comparison to saline group, as evidenced by that wounds in the Ajapocin-treated group were remarkably healed with a heal rate > 70 %, whereas 76 % of the wound areas remained in the saline-treated group (Fig. 8E). Hence, Ajapocin displayed distinct biological property associated with accelerating infected wound healing. Histopathological analysis (Fig. 8**F-G**) confirmed this fact that Ajapocin could enhance collagen deposition and accelerate re-epithelialization in wound closure. Taken together, these findings demonstrated that the potential of Ajapocin as an antimicrobial agent to help manage the *Vibrio* infections in clinical implementation.

4. Discussion

Vibrio species are classified as Class I pathogenic bacteria in aquaculture environment and public health [1,48,49]. Among them, *V. parahaemolyticus* and *V. vulnificus* serve as representative non-cholera pathogens, causing a range of infections and severe complications in susceptible individuals [2,5,50]. Despite recent centers for disease control and prevention (CDC) warnings on *Vibrio* infections [51], limited understanding of pathogenicity virulence, and the lack of systematic surveillance have hindered the development of effective countermeasures. AMPs are small molecules with potent activity in natural evolution [9], and several have shown promise in clinical translation due to their efficacy and membrane-targeting mechanisms, which are advantageous against antibiotic-resistant bacteria [52–54]. Given the challenges of treating *Vibrio* infections, marine-derived AMPs are particularly attractive because of their unique structural features and amino acid composition [14,55]. However, few marine AMPs have been explored for anti-*Vibrio* activity, underscoring the need for novel candidates.

In this study, we identified Ajapocin, a novel marine-sourced AMP, which exhibited potent antimicrobial activity against both *V. parahaemolyticus* and *V. vulnificus*, with rapid bactericidal effects within dozens of minutes. Ajapocin demonstrated efficacy in a zebrafish infection model and robust therapeutic effects in the *V. vulnificus*-infected mouse skin wound model. Mechanistically, Ajapocin disrupted bacterial membranes by enhancing permeability and inducing membrane depolarization. Importantly, it showed no cytotoxicity in

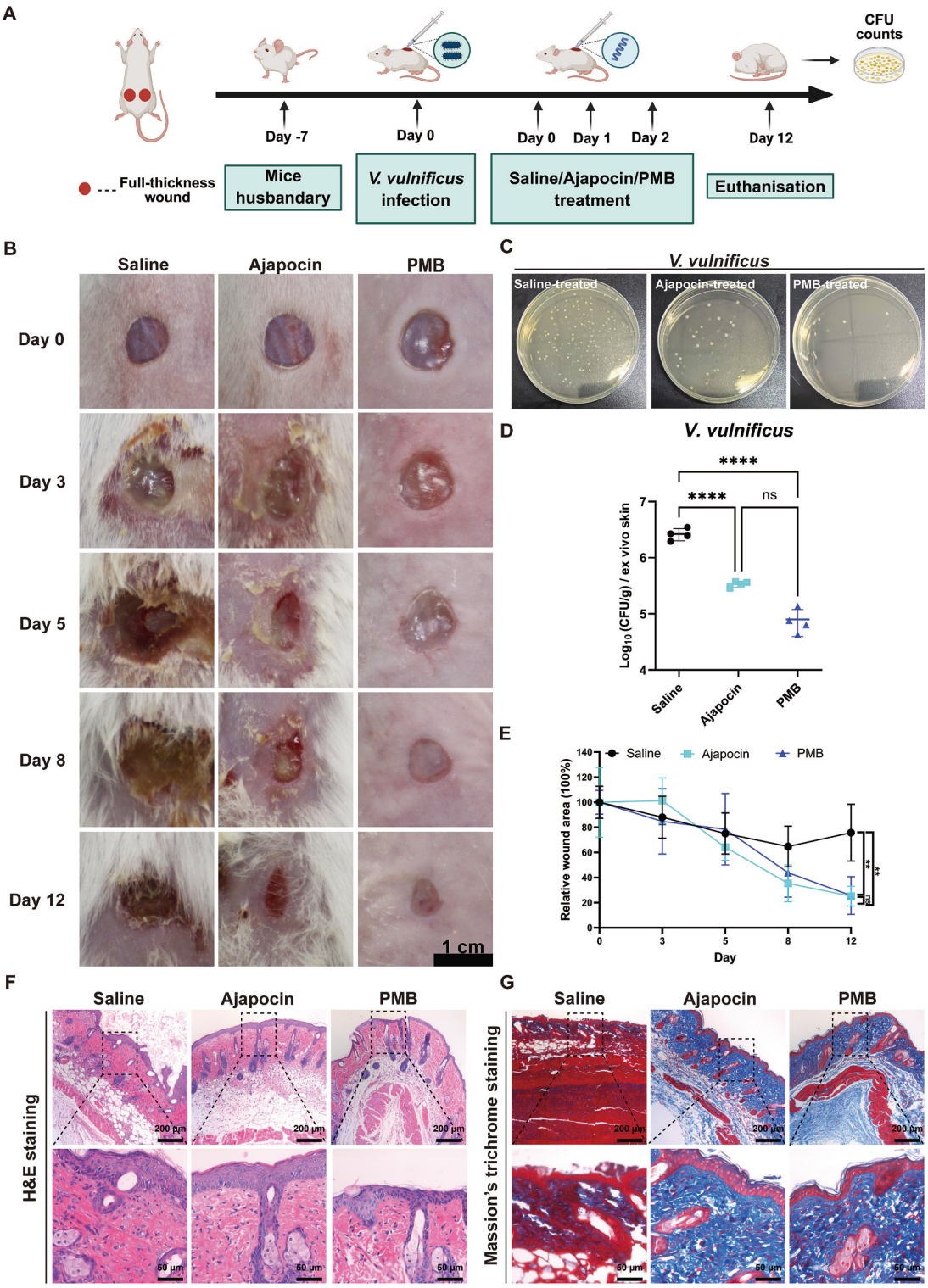

Fig. 8. Ajapocin exhibited potent therapeutic efficacy in a mouse wound infection model caused by *V. vulnificus*. (A) Schematic depiction of the sequence of mouse infection and treatment experiments. (B) Visual appearance of representative photographs of infected full-thickness wounds on saline-, Ajapocin- and PMB-treated groups. Scale bar, 1cm. (C) Images of *V. vulnificus* colonies grown on TSB agar plates after treatment with saline, Ajapocin and PMB. (D) Bacterial loads of *V. vulnificus* in saline-, Ajapocin- and PMB-treated wounds on day 12 post-treatment. $n = 4$ biologically independent animals. Statistical analysis was conducted using the Tukey's test: $^{****}P < 0.0001$. n.s. represented no significance. (E) Wound sizes of different treated groups on various days as a percentage of the initial wound size. $n = 4$ biologically independent samples. Statistical analysis was conducted using the Tukey's test: $^{**}P < 0.01$. n.s. represented no significance. (F) Representative images of wounds after treatment with saline, Ajapocin and PMB via H&E staining. Scale bars, 200 μm and 50 μm. (G) Representative images of wounds after treatment with saline, Ajapocin and PMB via Masson's trichrome staining. Scale bars, 200 μm and 50 μm.

mammalian cells and no cumulative *in vivo* toxicity following daily injection for a week, highlighting its translational potential.

To screen effective antimicrobial agents with robust activity against *V. parahaemolyticus* and *V. vulnificus* bacteria, we made our comprehensive consideration in peptide design, including cationic and amphiphilic features, coupled with structural conformation [56]. Activity assay confirmed that acquired Ajapocin exhibited excellent property to kill each *Vibrio*, moreover, it is noticeable that Ajapocin showed stronger effects than $Spgillcin_{177\text{-}189}$, another AMP derived from marine animal [57]. Notably, Ajapocin showed bactericidal potency comparable to PMB, a standard of care for Gram-negative bacteria, but without its associated renal toxicity [58]. Animal models further validated Ajapocin's therapeutic potential. In zebrafish models of *V. parahaemolyticus* and *V. vulnificus* infection, Ajapocin significantly improved survival (Fig. 7). In a murine wound healing (Fig. 8), demonstrating practical translational applicability [1,59]. Whereas the usage of PMB led to treatment failure in zebrafish-*Vibrio* infection model, probably this "last-resort" antibiotic bearing nephrotoxicity and neurotoxicity easily displayed toxic effects in the field of infection management. Therefore, a combination of high efficacy and low toxicity supports Ajapocin as a safer candidate for clinical application.

Given that superior performance of Ajapocin *in vitro* and *in vivo*, we undoubtedly uncover its molecular mechanism on *Vibrio* bacteria. We found that Ajapocin's action depended on membrane interactions, which is in consistent to mechanistic lysis profiles of most reported AMPs [54,60]. In addition, we further demonstrated that membrane-based potential target, we found that addition of LPS significantly attenuated antibacterial activity against each *Vibrio* strain, indicated Ajapocin was likely an LPS-targeting peptide [61], such as PMB. Differently, our results also revealed CL component abolished the potency of Ajapocin in mechanistic study. Both LPS and CL featured negative charge property and consisted of bacterial membrane [62], we concluded that membrane-interacting Ajapocin adopted membrane leakage profiles via electronic interaction. Additionally, antibiotic resistance of the isolated *Vibrios* is ongoing investigation, and emerging resistance to currently used antibiotics is a global public health crisis. Based on advanced treatment strategies, one sophisticated approach has been processed in screening or designing multi-target antimicrobials, which displayed the less prone to detectable resistance in the killing of pathogens. Ajapocin was identified a bifunctional molecule by acting on non-proteinaceous envelope targets, including both LPS and CL components, suggesting that Ajapocin could manifest its mechanistic advantage for combating antibiotic-resistant *Vibrio* pathogens in comparison to single-target antibiotic, such as PMB. Moreover, PC belongs to a neutral membrane component and mainly exist in mammalian cells [63], while Ajapocin-PC mixture had not blocked Ajapocin's activity in killing against *Vibrio* (Fig. 4**C-D**), meantime, which might be account for the selective effectiveness on bacteria not to cells and animals. Given that the precise results as shown in Fig. 3D, we demonstrated that Ajapocin showed superior effects than PMB in triggering membrane depolarization response. The reason for this phenomenon was closely associated with molecular mechanism. Based on physical–chemical characteristics, we acknowledged that Ajapocin featured high hydrophobicity (40 %) in nature and harbored helicity with α-helical conformation. On the basis of structure–activity relationship, Ajapocin adopting amphiphilic structure inserted the bacterial lipid bilayer, resulting in dramatic changes in membrane potential [64–66]. In contrast, the mechanism of action of PMB primarily involved an initial high-affinity interaction with the Lipid A component of LPS. Therefore, Ajapocin over PMB could exhibit stronger membrane depolarization effects although at same killing concentration.

There are some limitations remain. For example, we revealed the novel Ajapocin exhibited potent activity against *V. parahaemolyticus* and *V. vulnificus* pathogens. However, in addition to high-salinity tolerance, it is unclear that Ajapocin's ability in the presence of serum and proteolytic conditions. Next, we make our efforts to advance the systemic treatment regimen of Ajapocin in our follow-up studies. Mechanistic insights can be strengthened by biophysical studies, such as nuclear magnetic resonance (NMR) to probe interactions with LPS or CL [37]. Additionally, Ajapocin's efficacy in systemic infections, such as sepsis, has yet to be evaluated. Future work should explore these aspects to advance clinical translation.

4.1. Conclusion

In summary, we report a novel marine-sourced AMP, with cationic and α-helical features, exhibiting potent and rapid bactericidal activity against *V. parahaemolyticus* and *V. vulnificus*. Ajapocin displays *in vivo* efficacy in both zebrafish and *V. vulnificus*-infected mouse infection models through membranolytic mechanisms involving enhanced permeability and membrane depolarization. Its high antimicrobial activity combined with minimal toxicity highlights its promise as a therapeutic candidate. Future studies will focus on detailed mechanistic analysis and evaluation in systemic infection models to fully realize its clinical potential in combating *Vibrio* infections.

CRediT authorship contribution statement

Xiaofei Wang: Writing – original draft, Software, Methodology, Investigation, Funding acquisition. **Xiao Hong:** Writing – original draft, Supervision, Software, Methodology. **Wanting Liu:** Software, Methodology, Formal analysis. **Yujun Xu:** Software, Methodology. **Roushi Chen:** Software, Methodology. **Fangyi Chen:** Validation, Software, Funding acquisition, Formal analysis. **Ke-Jian Wang:** Writing – review & editing, Visualization, Validation, Resources, Funding acquisition, Formal analysis, Data curation, Conceptualization. **Luxi Wang:** Writing – review & editing, Writing – original draft, Visualization, Validation, Project administration, Funding acquisition, Data curation, Conceptualization.

Declaration of competing interest

The authors declare that they have no known competing financial interests or personal relationships that could have appeared to influence the work reported in this paper.

Acknowledgements

This study was financially supported by grant U1805233/32200620 from the National Natural Science Foundation of China; grant 25FV0CLZ09 from Fujian Ocean Innovation Center; grant FJHY-YYKJ-2024-2-3 from Fujian Ocean and Fisheries Bureau; and grant 22CZP002HJ08 from Xiamen Ocean Development Bureau. We meantime thank the Hui Peng and Zhiyong Lin for help in technological instruction.

Data availability

Data will be made available on request.

References

[1] C. Baker-Austin, J.D. Oliver, M. Alam, A. Ali, M.K. Waldor, F. Qadri, J. Martinez-Urtaza, Vibrio spp. infections, Nature Reviews Disease Primers 4(1) (2018) 1–19. doi:10.1038/s41572-018-0005-8.

[2] F.L. Thompson, T. Iida, J. Swings, Biodiversity of vibrios, Microbiol Mol Biol R 68 (3) (2004) 403, https://doi.org/10.1128/Mmbr.68.3.403-431.2004.

[3] M. Vandeputte, M.A. Kashem, P. Bossier, D. Vanrompay, *Vibrio* pathogens and their toxins in aquaculture: a comprehensive review, Rev Aquacult 16 (4) (2024) 1858–1878, https://doi.org/10.1111/raq.12926.

[4] T. Brauge, J. Mougin, T. Ells, G. Midelet, Sources and contamination routes of seafood with human pathogenic Vibrio spp.: A Farm-to-Fork approach, Compr Rev Food Sci F 23(1) (2024) 1–25. doi:10.1111/1541-4337.13283.

[5] C. Baker-Austin, J. Trinanes, N. Gonzalez-Escalona, J. Martinez-Urtaza, Non-Cholera Vibrios: the Microbial Barometer of climate Change, Trends Microbiol. 25 (1) (2017) 76–84, https://doi.org/10.1016/j.tim.2016.09.008.

[6] S. Elmahdi, L.V. DaSilva, S. Parveen, Antibiotic resistance of and in various countries: a review, Food Microbiol. 57 (2016) 128–134, https://doi.org/10.1016/j.fm.2016.02.008.

[7] K.C. Wong, A.M. Brown, G.M. Luscombe, S.J. Wong, K. Mendis, Antibiotic use for Vibrio infections: important insights from surveillance data, BMC Infect. Dis. 15 (2015), https://doi.org/10.1186/s12879-015-0959-z.

[8] N.J.r. Oliveira, C.M. Souza, D.F. Buccini, M.H. Cardoso, O.L. Franco, Antimicrobial peptides: structure, functions and translational applications, Nat. Rev. Microbiol. (2025), https://doi.org/10.1038/s41579-025-01200-y.

[9] B.P. Lazzaro, M. Zasloff, J. Rolff, Antimicrobial peptides: Application informed by evolution, Science 368 (6490) (2020) 487, https://doi.org/10.1126/science.aau5480.

[10] N. Mookherjee, M.A. Anderson, H.P. Haagsman, D.J. Davidson, Antimicrobial host defence peptides: functions and clinical potential, Nat. Rev. Drug Discov. 19 (5) (2020) 311–332, https://doi.org/10.1038/s41573-019-0058-8.

[11] C.R. Macnair, S.T. Rutherford, M.W. Tan, Alternative therapeutic strategies to treat antibiotic-resistant pathogens, Nat. Rev. Microbiol. 22 (5) (2024) 262–275, https://doi.org/10.1038/s41579-023-00993-0.

[12] I.Y. Park, J.H. Cho, K.S. Kim, Y.B. Kim, M.S. Kim, S.C. Kim, Helix stability confers salt resistance upon helical antimicrobial peptides, J. Biol. Chem. 279 (14) (2004) 13896–13901, https://doi.org/10.1074/jbc.M311418200.

[13] S.R. Xu, P. Tan, Q. Tang, T. Wang, Y.K. Ding, H.Y. Fu, Y.C. Zhang, C.L. Zhou, M. D. Song, Q.S. Tang, Z.H. Sun, X. Ma, Enhancing the stability of antimicrobial peptides: from design strategies to applications, Chem. Eng. J. 475 (2023), https://doi.org/10.1016/j.cej.2023.145923.

[14] S.V. Guryanova, S.V. Balandin, O.Y. Belogurova-Ovchinnikova, T.V. Ovchinnikova, Marine Invertebrate Antimicrobial Peptides and their potential as Novel Peptide Antibiotics, Mar. Drugs 21 (10) (2023), https://doi.org/10.3390/md21100503.

[15] R. Wu, J. Patocka, E. Nepovimova, P. Oleksak, M. Valis, W.D. Wu, K. Kuca, Marine Invertebrate Peptides: Antimicrobial Peptides, Front. Microbiol. 12 (2021), https://doi.org/10.3389/fmicb.2021.785085.

[16] M.A. Kawsar, C.Q. Zhao, F. Mao, Z.N. Yu, Y. Zhang, Unlocking Antimicrobial Peptides from Marine Invertebrates, A Comprehensive Review of Antimicrobial Discovery, Antibiotics-Basel 14 (9) (2025), https://doi.org/10.3390/antibiotics14090924.

[17] S.V. Sperstad, T. Haug, H.M. Blencke, O.B. Styrvold, C. Li, K. Stensvåg, Antimicrobial peptides from marine invertebrates: challenges and perspectives in marine antimicrobial peptide discovery, Biotechnol. Adv. 29 (5) (2011) 519–530, https://doi.org/10.1016/j.biotechadv.2011.05.021.

[18] A.J. Otero-González, B.S. Magalhaes, M. Garcia-Villarino, C. López-Abarrategui, D. A. Sousa, S.C. Dias, O.L. Franco, Antimicrobial peptides from marine invertebrates as a new frontier for microbial infection control, FASEB J. 24 (5) (2010) 1320–1334, https://doi.org/10.1096/fj.09-143388.

[19] T. Rodrigues, F.A. Guardiola, D. Almeida, A. Antunes, Aquatic Invertebrate Antimicrobial Peptides in the fight against Aquaculture Pathogens, Microorganisms 13 (1) (2025), https://doi.org/10.3390/microorganisms13010156.

[20] H. Fedders, M. Michalek, J. Groetzinger, M. Leippe, An exceptional salt-tolerant antimicrobial peptide derived from a novel gene family of haemocytes of the marine invertebrate, Biochem. J 416 (2008) 65–75, https://doi.org/10.1042/Bj20080398.

[21] W.J. Xian, M.R. Hennefarth, M.W. Lee, T. Do, E.Y. Lee, A.N. Alexandrova, G.C. L. Wong, Histidine-Mediated Ion specific Effects Enable Salt Tolerance of a Pore-Forming Marine Antimicrobial Peptide, Angew. Chem. Int. Edit. 61 (25) (2022), https://doi.org/10.1002/anie.202108501.

[22] P. Schmitt, R.D. Rosa, D. Destoumieux-Garzón, An intimate link between antimicrobial peptide sequence diversity and binding to essential components of bacterial membranes, BBA-Biomembranes 1858 (5) (2016) 958–970, https://doi.org/10.1016/j.bbamem.2015.10.011.

[23] J. Jo, J. Oh, H.G. Lee, H.H. Hong, S.G. Lee, S. Cheon, E.M.A. Kern, S. Jin, S.J. Cho, J.K. Park, C. Park, Draft genome of the sea cucumber and genetic polymorphism among color variants (vol 6, pg 1, 2017), Gigascience 6(10) (2017). doi:10.1093/gigascience/gix069.

[24] L.A. Sun, C.X. Jiang, F. Su, W. Cui, H.S. Yang, Chromosome-level genome assembly of the sea cucumber Apostichopus japonicus, Sci. Data 10 (1) (2023), https://doi.org/10.1038/s41597-023-02368-9.

[25] G. Wang, C. Schmidt, X. Li, Z. Wang, APD6: the antimicrobial peptide database is expanded to promote research and development by deploying an unprecedented information pipeline, Nucleic Acids Res. (2025), https://doi.org/10.1093/nar/gkaf860.

[26] U. Gawde, S. Chakraborty, F.H. Waghu, R.S. Barai, A. Khanderkar, R. Indraguru, T. Shirsat, S. Idicula-Thomas, $CAMP_{R4}$: a database of natural and synthetic antimicrobial peptides, Nucleic Acids Res. 51 (D1) (2023) D377–D383, https://doi.org/10.1093/nar/gkac933.

[27] P.N. Paqué, L. Karygianni, J. Kneubuehler, L. Fiscalini, D.B. Wiedemeier, M. Müller, T. Attin, T. Thurnheer, Microbial approaches for the assessment of toothpaste efficacy against oral species: a method comparison, Microbiologyopen 11 (2) (2022), https://doi.org/10.1002/mbo3.1271.

[28] Z.Q. Wang, B. Koirala, Y. Hernandez, M. Zimmerman, S.F. Brady, Bioinformatic prospecting and synthesis of a bifunctional lipopeptide antibiotic that evades resistance, Science 376 (6596) (2022) 991, https://doi.org/10.1126/science.abn4213.

[29] J. Zhang, L. Luan, Y. Xu, S. Jiang, W. Zhang, L. Tian, W. Ye, J. Han, C. Zhang, T. Wang, Q. Meng, Development of novel broad-spectrum amphipathic antimicrobial peptides against multidrug-resistant bacteria through a rational combination strategy, J. Adv. Res. (2025), https://doi.org/10.1016/j.jare.2025.01.029.

[30] J. Mwangi, Y.Z. Yin, G. Wang, M. Yang, Y. Li, Z.Y. Zhang, R. Lai, The antimicrobial peptide ZY4 combats multidrug-resistant *Pseudomonas aeruginosa* and *Acinetobacter baumannii* infection, P Natl Acad Sci USA 116 (52) (2019) 26516–26522, https://doi.org/10.1073/pnas.1909585117.

[31] H.D. Zhang, Q. Chen, J.Y. Xie, Z.H. Cong, C.T. Cao, W.J. Zhang, D.H. Zhang, S. Chen, J.W. Gu, S. Deng, Z.Q. Qiao, X.Y. Zhang, M.Q. Li, Z.Y. Lu, R.H. Liu, Switching from membrane disrupting to membrane crossing, an effective strategy in designing antibacterial polypeptide, Sci. Adv. 9 (4) (2023), https://doi.org/10.1126/sciadv.abn0771.

[32] J.Y. Xie, M. Zhou, Z.H. Cong, X.M. Xiao, L.Q. Liu, S. Chen, W.A. Jiang, Y.M. Wu, R. H. Liu, A host defense peptide-mimicking prodrug activated by drug-resistant Gram-negative bacterial infections, Sci. Transl. Med. 17 (801) (2025), https://doi.org/10.1126/scitranslmed.adl4870.

[33] M.R. Song, Y. Liu, X.Y. Huang, S.Y. Ding, Y. Wang, J.Z. Shen, K. Zhu, A broad-spectrum antibiotic adjuvant reverses multidrug-resistant Gram-negative pathogens, Nat. Microbiol. 5 (8) (2020) 1040, https://doi.org/10.1038/s41564-020-0723-z.

[34] J.R. Shi, C. Chen, D.J. Wang, Z.Q. Wang, Y. Liu, The antimicrobial peptide LI14 combats multidrug-resistant bacterial infections, Commun Biol 5(1) (2022). doi: 10.1038/s42003-022-03899-4.

[35] Y. Yang, F.Y. Chen, H.Y. Chen, H. Peng, H. Hao, K.J. Wang, A Novel Antimicrobial Peptide Scyreprocin from Mud Crab showing Potent Antifungal and Anti-biofilm activity, Front. Microbiol. 11 (2020), https://doi.org/10.3389/fmicb.2020.01589.

[36] X.Y. Chen, M.R. Song, L. Tian, X.X. Shan, C.S. Mao, M.H. Chen, J.Q. Zhao, A. Sami, H.Q. Yin, U. Ali, J.W. Shi, H.H. Li, Y.Q. Zhang, J.H. Zhang, S.X. Wang, C.L. Shi, Y. H. Chen, X.D. Du, K. Zhu, L.J. Wu, A plant peptide with dual activity against multidrug-resistant bacterial and fungal pathogens, Sci. Adv. 11 (12) (2025), https://doi.org/10.1126/sciadv.adt8239.

[37] D. Nagarajan, N. Roy, O. Kulkarni, N. Nanajkar, A. Datey, S. Ravichandran, C. Thakur, T. Sandeep, I.V. Aprameya, S.P. Sarma, D. Chakravortty, N. Chandra, Ω76: a designed antimicrobial peptide to combat carbapenem- and tigecycline-resistant, Sci. Adv. 5 (7) (2019), https://doi.org/10.1126/sciadv.aax1946.

[38] X.X. Song, Z. Zhou, A. Elmezayen, R.L. Wu, C.H. Yu, B.N. Gao, J.D. Minna, K. D. Westover, H.J. Zeh, G. Kroemer, L.E. Heasley, R. Kang, D.L. Tang, SRC kinase drives multidrug resistance induced by KRAS-G12C inhibition, Sci. Adv. 10 (50) (2024), https://doi.org/10.1126/sciadv.adq4274.

[39] J.L. Narayana, B. Mishra, T. Lushnikova, Q.H. Wu, Y.S. Chhonker, Y.X. Zhang, D. Zarena, E.S. Salnikov, X.L. Dang, F.Y. Wang, C. Murphy, K.W. Foster, S. Gorantla, B. Bechinger, D.J. Murry, G.S. Wang, Two distinct amphipathic peptide antibiotics with systemic efficacy, P Natl Acad Sci USA 117 (32) (2020) 19446–19454, https://doi.org/10.1073/pnas.2005540117.

[40] J. Li, M.J. Liu, W.J. Du, X.L. Peng, H. Deng, H.X. Zi, H.B. Shang, J.L. Du, Neural-activity-regulated and glia-mediated control of brain lymphatic development, Cell 188 (12) (2025), https://doi.org/10.1016/j.cell.2025.04.008.

[41] V. Torraca, S. Mostowy, Zebrafish Infection: from Pathogenesis to Cell Biology, Trends Cell Biol. 28 (2) (2018) 143–156, https://doi.org/10.1016/j.tcb.2017.10.002.

[42] P.K. Hazam, C.C. Cheng, W.C. Lin, C.Y. Hsieh, P.H. Hsu, Y.R. Chen, C.C. Li, P. R. Hsueh, J.Y. Chen, Strategic modification of low-activity natural antimicrobial peptides confers antibacterial potential in vitro and in vivo, Eur. J. Med. Chem. 249 (2023), https://doi.org/10.1016/j.ejmech.2023.115131.

[43] C. Ntallis, N.I. Martin, A.M. Edwards, M. Weingarth, Bacterial cell envelope-targeting antibiotics, Nat. Rev. Microbiol. (2025), https://doi.org/10.1038/s41579-025-01247-x.

[44] C. Sohlenkamp, O. Geiger, Bacterial membrane lipids: diversity in structures and pathways, FEMS Microbiol. Rev. 40 (1) (2016) 133–159, https://doi.org/10.1093/femsre/fuv008.

[45] J.N. van der Veen, J.P. Kennelly, S. Wan, J.E. Vance, D.E. Vance, R.L. Jacobs, The critical role of phosphatidylcholine and phosphatidylethanolamine metabolism in health and disease, BBA-Biomembranes 1859 (9) (2017) 1558–1572, https://doi.org/10.1016/j.bbamem.2017.04.006.

[46] H.Q. Zhang, C.B. Sun, N. Xu, W.S. Liu, The current landscape of the antimicrobial peptide melittin and its therapeutic potential, Front. Immunol. 15 (2024), https://doi.org/10.3389/fimmu.2024.1326033.

[47] S.N. Avedissian, J.J. Liu, N.J. Rhodes, A. Lee, G.M. Pais, A.R. Hauser, M.H. Scheetz, A Review of the Clinical Pharmacokinetics of Polymyxin B, Antibiotics-Basel 8(1) (2019). doi:10.3390/antibiotics8010031.

[48] T.M. Bartlett, B.P. Bratton, A. Duvshani, A. Miguel, Y. Sheng, N.R. Martin, J. P. Nguyen, A. Persat, S.M. Desmarais, M.S. VanNieuwenhze, K.C. Huang, J. Zhu, J. W. Shaevitz, Z. Gitai, A Periplasmic Polymer Curves Vibrio cholerae and Promotes Pathogenesis, Cell 168 (1–2) (2017) 172, https://doi.org/10.1016/j.cell.2016.12.019.

[49] M. Liu, H. Wang, Z. Wang, H. Wang, K. Zhang, J. Xue, R.H. Liu, Y. Liu, P.Y. Xia, H. Wang, B. Kan, Y. Li, S. Li, Y. Fu, A *Vibrio*-specific T6SS effector reshapes microbial competition by disrupting bioenergetics, Cell Host Microbe 33 (7) (2025), https://doi.org/10.1016/j.chom.2025.06.001.

[50] S.K. Banerjee, J.M. Farber, Trend and Pattern of Antimicrobial Resistance in Molluscan Vibrio Species Sourced to Canadian Estuaries, Antimicrob Agents Ch 62 (10) (2018), https://doi.org/10.1128/AAC.00799-18.

[51] E. Harris, CDC Issues Warning amid Vibrio vulnificus Infections, Jama-J Am Med Assoc 330 (14) (2023) 1318, https://doi.org/10.1001/jama.2023.17816.

[52] C. Ghosh, P. Sarkar, R. Issa, J. Haldar, Alternatives to conventional Antibiotics in the Era of Antimicrobial Resistance, Trends Microbiol. 27 (4) (2019) 323–338, https://doi.org/10.1016/j.tim.2018.12.010.
[53] J.Q. Xuan, W.G. Feng, J.Y. Wang, R.C. Wang, B.W. Zhang, L.T. Bo, Z.S. Chen, H. Yang, L.M. Sun, Antimicrobial peptides for combating drug-resistant bacterial infections, Drug Resist Update 68 (2023), https://doi.org/10.1016/j.drup.2023.100954.
[54] A. de Breij, M. Riool, R.A. Cordfunke, N. Malanovic, L. de Boer, R.I. Koning, E. Ravensbergen, M. Franken, T. van der Heijde, B.K. Boekema, P.H.S. Kwakman, N. Kamp, A. El Ghalbzouri, K. Lohner, S.A.J. Zaat, J.W. Drijfhout, P.H. Nibbering, The antimicrobial peptide SAAP-148 combats drug-resistant bacteria and biofilms, Sci. Transl. Med. 10 (423) (2018), https://doi.org/10.1126/scitranslmed.aan4044.
[55] R. Ribeiro, E. Pinto, C. Fernandes, E. Sousa, Marine Cyclic Peptides: Antimicrobial activity and Synthetic strategies, Mar. Drugs 20 (6) (2022), https://doi.org/10.3390/md20060397.
[56] A.T. Tucker, S.P. Leonard, C.D. DuBois, G.A. Knauf, A.L. Cunningham, C.O. Wilke, M.S. Trent, B.W. Davies, Discovery of Next-Generation Antimicrobials through Bacterial Self-Screening of Surface-Displayed Peptide Libraries, Cell 172 (3) (2018) 618, https://doi.org/10.1016/j.cell.2017.12.009.
[57] X.F. Wang, X. Hong, F.Y. Chen, K.J. Wang, A truncated peptide $Spgillcin_{177\text{-}189}$ derived from mud crab exerting multiple antibacterial activities, Front Cell Infect Mi 12 (2022), https://doi.org/10.3389/fcimb.2022.928220.
[58] X.F. Liu, Y.C. Chen, H.J. Yang, J. Li, J.C. Yu, Z.W. Yu, G.Y. Cao, X.J. Wu, Y. Wang, H.L. Wu, Y.X. Fan, J.J. Wang, J.F. Wu, Y. Jin, B.N. Guo, J.L. Hu, X.C. Bian, X. Li, J. Zhang, Acute toxicity is a dose-limiting factor for intravenous polymyxin B: a safety and pharmacokinetic study in healthy chinese subjects, J Infection 82 (2) (2021) 207–215, https://doi.org/10.1016/j.jinf.2021.01.006.
[59] M.A. Horseman, S. Surani, A comprehensive review of Vibrio vulnificus: an important cause of severe sepsis and skin and soft-tissue infection, Int. J. Infect. Dis. 15 (3) (2011) E157–E166, https://doi.org/10.1016/j.ijid.2010.11.003.
[60] B. Ma, C. Fang, L.S. Lu, M.Z. Wang, X.Y. Xue, Y. Zhou, M.K. Li, Y. Hu, X.X. Luo, Z. Hou, The antimicrobial peptide thanatin disrupts the bacterial outer membrane and inactivates the NDM-1 metallo-β-lactamase, Nat. Commun. 10 (2019), https://doi.org/10.1038/s41467-019-11503-3.
[61] A. Basauri, C. González-Fernández, M. Fallanza, E. Bringas, R. Fernandez-Lopez, L. Giner, G. Moncalián, F. de la Cruz, I. Ortiz, Biochemical interactions between LPS and LPS-binding molecules, Crit. Rev. Biotechnol. 40 (3) (2020) 292–305, https://doi.org/10.1080/07388551.2019.1709797.
[62] Y.L. Sun, Z.X. Deng, X.K. Jiang, B. Yuan, K. Yang, Interactions between polymyxin B and various bacterial membrane mimics: a molecular dynamics study, Colloid Surface B 211 (2022), https://doi.org/10.1016/j.colsurfb.2021.112288.
[63] Z. Cui, M. Houweling, Phosphatidylcholine and cell death, BBA-Mol. Cell Biol. L. 1585 (2–3) (2002) 87–96, https://doi.org/10.1016/S1388-1981(02)00328-1.
[64] D. Saeloh, V. Tipmanee, K.K. Jim, M.P. Dekker, W. Bitter, S.P. Voravuthikunchai, M. Wenzel, L.W. Hamoen, The novel antibiotic rhodomyrtone traps membrane proteins in vesicles with increased fluidity, PLoS Pathog. 14 (2) (2018), https://doi.org/10.1371/journal.ppat.1006876.
[65] W. Kim, G.J. Zou, T.P.A. Hari, I.K. Wilt, W.P. Zhu, N. Galle, H.A. Faizi, G. L. Hendricks, K. Tori, W. Pan, X.W. Huang, A.D. Steele, E.E. Csatary, M. M. Dekarske, J.L. Rosen, N.D. Ribeiro, K. Lee, J. Port, B.B. Fuchs, P.M. Vlahovska, W.M. Wuest, H.J. Gao, F.M. Ausubel, E. Mylonakis, A selective membrane-targeting repurposed antibiotic with activity against persistent methicillin-resistant Staphylococcus aureus, P Natl Acad Sci USA 116 (33) (2019) 16529–16534, https://doi.org/10.1073/pnas.1904700116.
[66] M.A. Farha, C.P. Verschoor, D. Bowdish, E.D. Brown, Collapsing the Proton Motive Force to Identify Synergistic Combinations against taphylococcus aureus, Chem. Biol. 20 (9) (2013) 1168–1178, https://doi.org/10.1016/j.chembiol.2013.07.006.